



HAL
open science

Experimental testing of school furniture designed with life-saving functions in case of earthquakes

Martina Sciomenta, Gabriele Tamagnone, Laura Gioiella, Fabio Micozzi, Alessandro Zona, Andrea Dall'asta, Massimo Fragiaco

► **To cite this version:**

Martina Sciomenta, Gabriele Tamagnone, Laura Gioiella, Fabio Micozzi, Alessandro Zona, et al.. Experimental testing of school furniture designed with life-saving functions in case of earthquakes. *Engineering Structures*, 2025, Nonstructural Elements in Buildings and Seismic Resilience, 336, pp.120389. <10.1016/j.engstruct.2025.120389>. <hal-05165626>

HAL Id: hal-05165626

<https://hal.science/hal-05165626v1>

Submitted on 16 Jul 2025

HAL is a multi-disciplinary open access archive for the deposit and dissemination of scientific research documents, whether they are published or not. The documents may come from teaching and research institutions in France or abroad, or from public or private research centers.

L'archive ouverte pluridisciplinaire **HAL**, est destinée au dépôt et à la diffusion de documents scientifiques de niveau recherche, publiés ou non, émanant des établissements d'enseignement et de recherche français ou étrangers, des laboratoires publics ou privés.



Distributed under a Creative Commons CC BY-NC 4.0 - Attribution - Non-commercial use - International License

21 **Keywords:** *Earthquake-resistant non-structural components, seismic design, life-saving furniture,*
22 *destructive furniture tests, furniture ultimate load-carrying capacity*

23 **1 Introduction**

24 In the past two decades earthquakes in Italy revealed significant vulnerabilities within the country's
25 building stock, especially in buildings with public functions, like schools. The tragic collapse of a
26 school in San Giuliano di Puglia in October 2002, due to a 5.8 magnitude earthquake, resulted in the
27 death of 27 children and teachers [1]. The L'Aquila earthquake in 2009, with a 5.9 magnitude, was
28 particularly devastating, causing 309 fatalities and leaving 1,600 people injured. The university
29 residence collapsed, alone resulting in eight casualties [2,3]. The Central Italy earthquakes in
30 August 2016 (magnitude 6.2), October 2016 (magnitude 6.6), and January 2017 (magnitude 5.7)
31 caused 300 fatalities, injuries and severe damage in the constructions, including schools and the
32 heritage buildings of the University of Camerino. These disasters underscored the susceptibility of
33 public buildings to seismic events. Reports, such as the [4,5], noted that many educational facilities
34 at all levels were severely damaged and condemned. Braga et al. [6] discussed on the extensive non-
35 structural elements' damage in RC buildings, which can vary from small cracks to collapse,
36 pointing the attention on the role those elements played in the overall safety assessment, socio-
37 economic framework, including human casualties and loss of building functionality. Same issues
38 can be caused by other non-structural components such furniture, which overturning or motion can
39 cause serious injuries to people and make the evacuation action even more difficult [7,8]. Materials
40 and analytical methods aiming to describe components' performances were largely investigated [9-
41 11]. However, the shape is crucial in some situations, since it allows to employ furniture as a
42 temporary shelter, thanks to the chance to create a survival triangle. Often, such behaviour is merely
43 coincidental, rather than a result of a deliberate design for life-saving functions.

44 If attention is focused on school furniture, different proposals for school desks able to resist vertical
45 impacts can be found: the award-winning Earthquake Desk designed by Arthur Brutter and Ido
46 Bruno made of steel and birch plywood able to resist to a 422 kg weight dropped on its tabletop
47 [12], the metal desk developed by an American company (LifeGuard Structures [13]), and Lifeshell
48 [14] entirely made of cross-laminated timber. However, such products are much heavier and more
49 expensive than regular school desks, making unlikely their actual diffusion in schools. In addition,
50 school desks are only one of the elements in the furniture of a classroom. An effective way to
51 protect pupils requires a broader approach, where all furniture elements should be conceived as
52 coordinated products able to provide shelter in the case of damage and failure in the building.

53 **2 Objectives and methods**

54 In this work, the possibility to turn non-structural components, specifically school furniture, into
55 lifesaving shields in case of earthquake event is investigated. The idea was to start from traditional
56 school desks and self-supporting shelving units, currently compliant with the intended use
57 standards, modifying them, in design as well as in performance, to enhance products with structural
58 load-bearing features. All the development process phases to obtain ready-to-use commercial
59 products are hereafter exposed and discussed [15,16].

60 A further novel purpose provided to the state of the art of the technical and scientific literature by
61 the present research is represented by the test protocols. This holistic methodology could be useful
62 to designers and furniture companies interested in the development of earthquake-proof furniture
63 for the school and office sectors as well as to the standard committee which could account for those
64 tests in the next regulatory update.

65 For both the desk and the self-supporting shelving unit, the process started with the item
66 conceptualisation, to respond to usability and standardised geometry criteria imposed by the norm.
67 This step was then followed by a design phase aimed at incorporating specific features enabling the

68 specimens to provide the sought additional safety and resistance in case of earthquake. Both objects
69 underwent finite elements analyses which gave a rough estimation of the expected capacity and
70 helped to further refine the concepts. After the prototyping phase, where the partner companies
71 were asked to produce specimens as close as possible to the set geometrical requirements,
72 considering their present manufacturing process, the two proposed furniture solutions were
73 subjected to different testing protocols devised to assess the effectiveness of the new designs. After
74 that, an optimisation phase allowed to fix certain problems encountered during the tests and build
75 better elements, which were then tested in a final experimental campaign.

76 **3 School desks**

77 **3.1 Conceptualization**

78 *3.1.1 Traditional school desk*

79 Traditional school desks are conceived to host students and equipment and are produced to meet the
80 dimensional requirements of EN 1729-1 and the safety function of EN 1729-2. Focusing on this
81 work, two traditional desks produced by two different partner companies, one labelled with the
82 letter “V” and the other with the letter “S”, having different shapes and geometrical features, were
83 accounted in the experimental campaign to diversify their performances and compare them with the
84 life-saving ones. Despite the differences (summarized on Table 1), the design and production
85 process of the two desks is essentially the same: they were realized with tube-shaped legs mutually
86 connected via welded joints to the horizontal perimetral frame at the top. The tabletops are made of
87 two of the most widely used materials: *(i)* particleboards (PB), an agglomerate of wood particles
88 and glue with very low shear resistance, and *(ii)* veneer boards (VB), which is made of wood ply,
89 normally up to 3 mm thick, overlapped and glued together. Although the latter solution provides

90 better characteristics, these types of boards are meant to perform best for in-plane loads, meaning an
91 out of plane concentrated load could damage severely the top.

92 3.1.2 *Life-saving school desk*

93 School desks are simple objects that can be made resistant to falling masses in the case of seismic
94 damage through an oversizing of all its components, as can be found in many examples. However,
95 the oversizing path produces school desks that are impractical in everyday use, being very heavy to
96 arrange in the different configurations required by a given class, and commonly very expensive,
97 thus, unaffordable by public administrations managing schools. To overcome these limitations, in
98 the study here presented, a different approach was followed: instead of using oversized elements
99 arranged into conventional desk shapes, elements commonly used for traditional school desk
100 constitute an innovative desk shape able to emphasize structural performance. The main novelties of
101 the proposed desk compared to the traditional one (Figure 1) are: (i) a 1 mm thick steel sheet,
102 fastened to the bottom side of the tabletop; (ii) an external frame (made teal tube-shaped profiles
103 with diameter 22 mm and thickness 1.5 mm) providing direct support to the tabletop and an inner
104 frame with similar geometry connected to the outer frame at the four corners and at the basis, along
105 the shorter sides of the desk.

106 Specifically, the inner frame provides support to the outer frame, collaborates towards a progressive
107 bending damage in case of strong overloading (being the larger inclination of the legs of the inner
108 frame properly optimized for this task), improves overall stability, and provides a backing
109 protection in case of damage/failure in the upper part. The steel sheet was added to prevent possible
110 brittle failure of the tabletop, typical of non-structural timber panels.

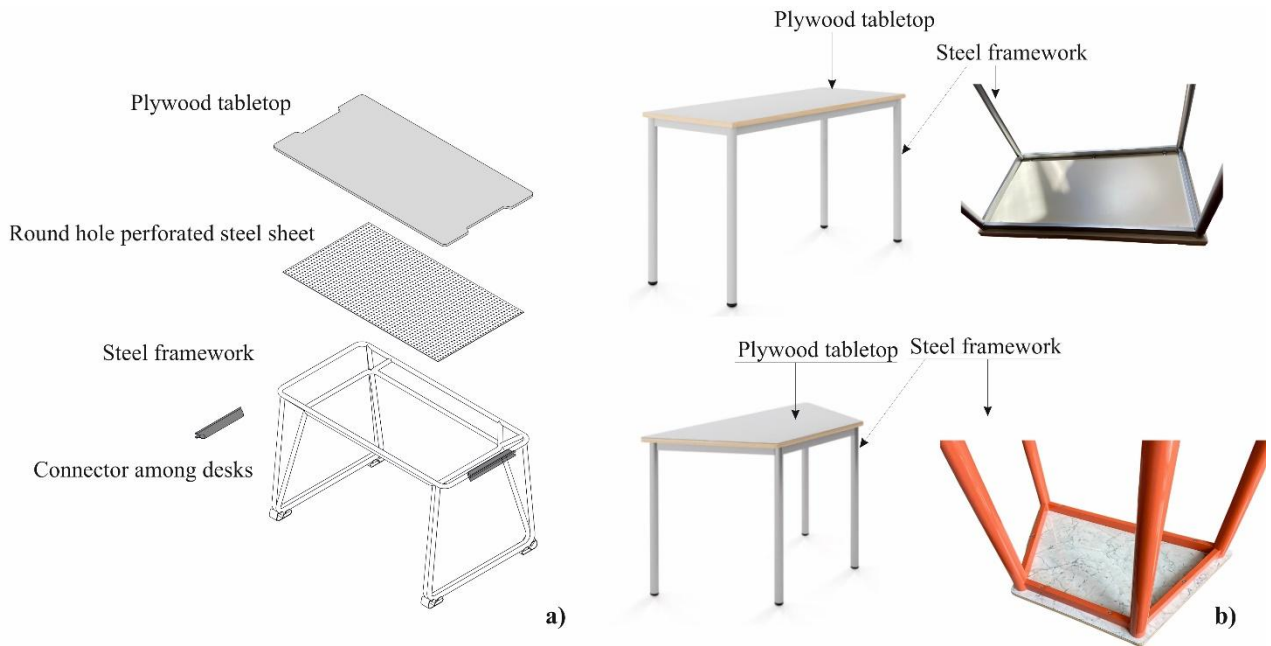
111 The resulting desk is much lighter if compared to other proposed earthquake-proof desks, more
112 economical, being based on materials, sections, dimensions of elements and manufacturing
113 processes already adopted in common desks, does not have moving components that could harm

114 users, and has a bending-dominated damage in case of significant overloading that exploits the
 115 ductility of steel to dissipate impact energy while preserving the volume of the protection area.

116 The most relevant geometrical features of the tested specimens are summarized on Table 1,
 117 including their weight. For sake of comparison, it is worth mentioning the weight of other life-
 118 saving desks available in literature: the Lifeshell desk made of CLT elements has a weight of 119
 119 kg, while the Earthquake Desk designed by Arthur Brutter and Ido Bruno made of steel frame and
 120 birch plywood tabletop weights 25 kg (sized to host two students).

121 **Table 1.** Traditional and life-saving desk geometrical dimensions and shapes

Specimen	Type	Shape	B [m]	b [m]	h [m]	H [m]	Tabletop area [m ²]	Weight [kg]
	Traditional		1,1	1,1	0,6	0,75	0,66	15
V series	Proposed life- saving	Rectangular	1,1	1,1	0,6	0,75	0,66	18
	Traditional		0,88	0,51	0,5	0,75	0,35	14.8
S series	Proposed life- saving	Trapezoid	1,1	0,72	0,5	0,78	0,46	18

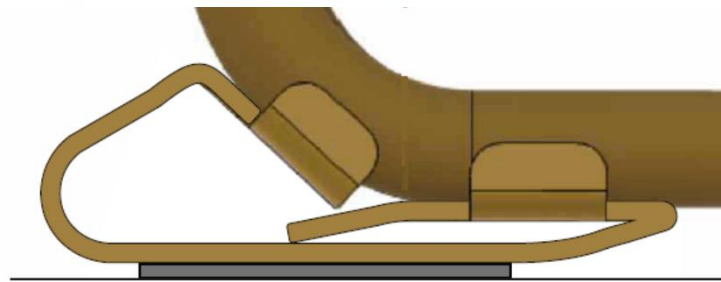


122

123 **Figure 1.** School desk structure: **a)** Proposed life-saving; **b)** Traditional (rectangular and trapezoidal versions)

124 After the first experimental campaign, the desks' structure was optimized, in particular: (i) the
 125 under table steel sheet was replaced with a round hole, perforated, version with the same thickness;
 126 the aim was to lighten the desks without lose the anti-intrusion function; (ii) four collapsible steel
 127 feet, made of 3 mm thick metal sheet, were added to dissipate energy in case of impact (Figure 2).

128



129 **Figure 2.** Proposed dissipative foot

130 Additional optimization operations were carried out after the second impact test campaign, with the
 131 welding of additional reinforcement elements (Figure 3) to connect the inner and the outer frame, to
 132 efficiently re-distribute the vertical loads and reducing the deflections in bending of the inner frame
 133 tube elements.

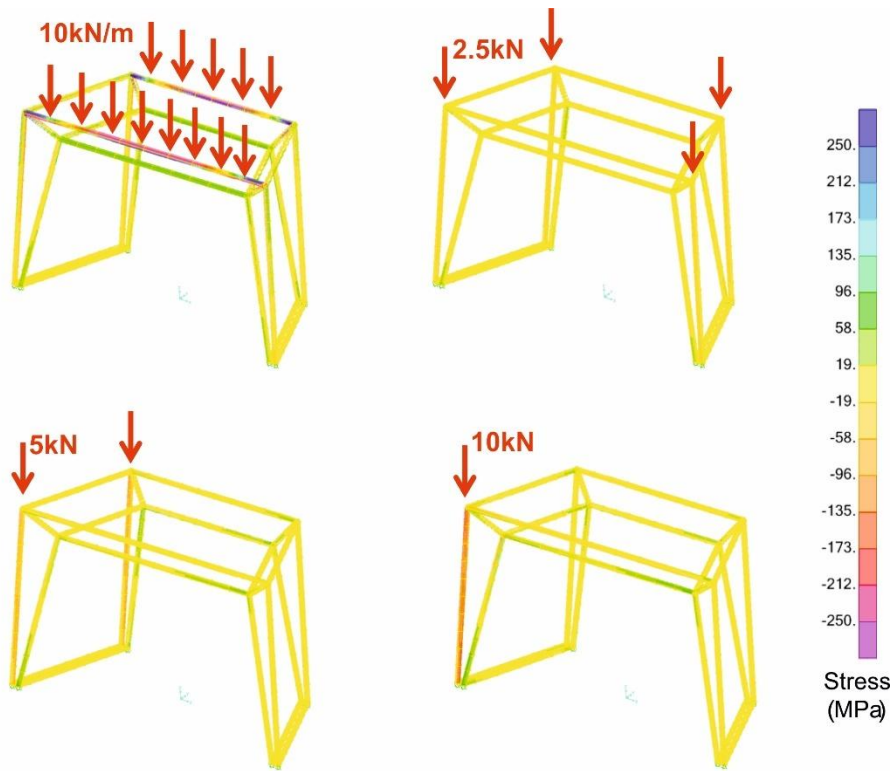


134

135 **Figure 3.** Welded elements connecting the inner and outer frames

136 **3.2 Preliminary design via numerical simulation**

137 Recent studies investigated the seismic design [17] and modelling [18] of inelastic non-structural
138 elements, providing insights into their strength-reduction factors and response under building floor
139 motions. In this framework, the shape of the school desk was optimized considering vertical
140 distributed and concentrated loads, both symmetric and non-symmetric, through a finite element
141 model implemented in the SAP 2000 software (Figure 4). The most critical loading condition was
142 identified as a concentrated force at one corner with global stability being the most demanding
143 verification. However, this preliminary numerical study could only provide initial indications, with
144 impact tests needed for deeper insight.



145

146 **Figure 4.** Examples of preliminary numerical simulations for the design of the proposed life-saving school desk

147 3.3 Prototyping and tests

148 After the preliminary numerical analyses, the proposed life-saving components were pre-
 149 dimensioned and prototyped. It is worth highlighting that the two industrial partners, in compliance
 150 with the suggested measures, manufactured their products autonomously, based on their equipment,
 151 know-how and stocks, so their products could slightly differ from each other's and from the design
 152 features for some processing details and dimensions, and which influence will be hereafter
 153 explained.

154 Since the accredited tests for school furniture strength and safety (EN 1729-2:2023 for chairs and
 155 tables in educational institutions, EN 16121:2023 for non-domestic storage furniture) consider loads
 156 and protocols consistent with their operational functions, in this work, non-standard test methods
 157 were proposed and applied to experimentally evaluate the capacity to resist overloading as that
 158 expected in the case of damage following seismic events.

159 The experimental campaign was carried out at the laboratory of the Department of Civil,
160 Construction-Architectural and Environmental Engineering (DICEAA) of the University of
161 L'Aquila. Two different types of tests were carried out on the proposed life-saving school desks: (i)
162 monotonic static tests with both concentrated and distributed load (with and without eccentricity) to
163 test the punching shear capacity of tabletop and the load bearing capacity of the steel frame,
164 respectively; and (ii) dynamic (impact) tests to establish the overall load-bearing behaviour if debris
165 detachment from the ceiling occur.

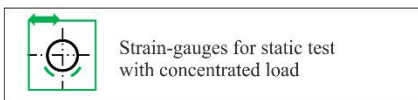
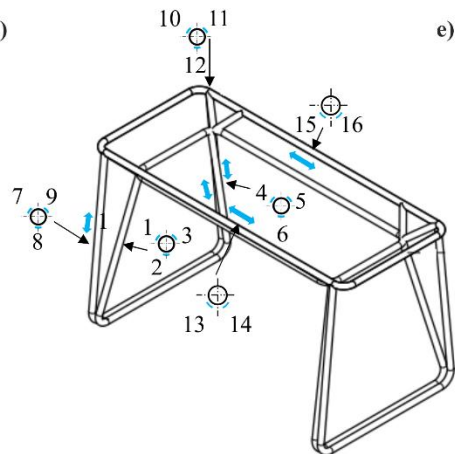
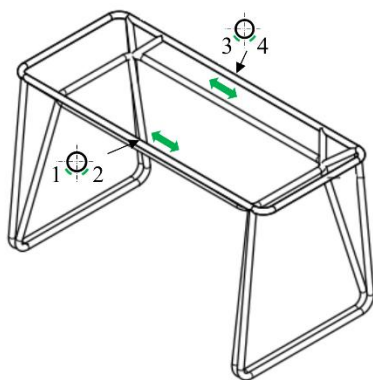
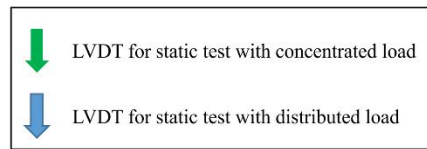
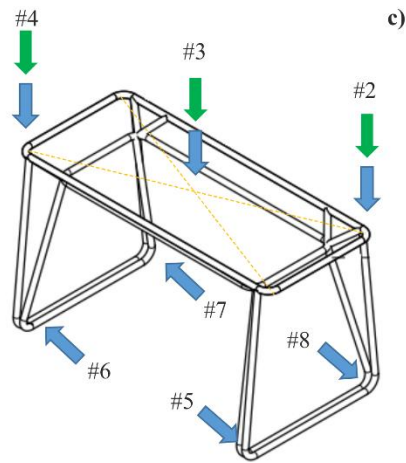
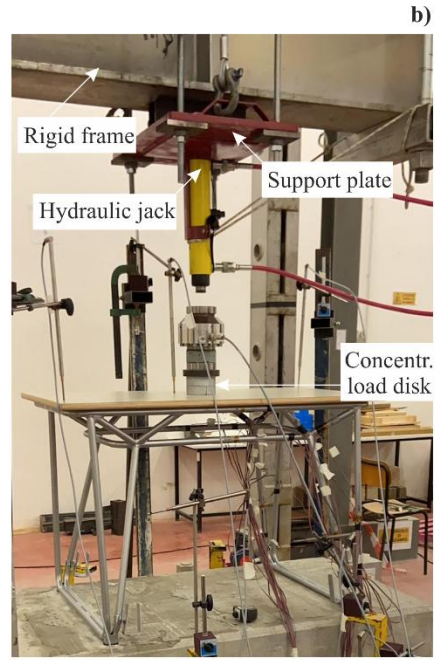
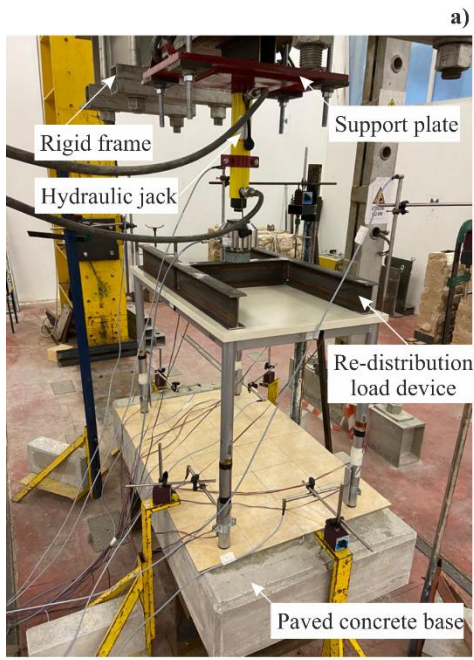
166 According to Section 2, two subsequent test campaigns were carried out: during the first, static
167 monotonic and impact tests were performed to compare the performances of life-saving innovative
168 desks with those of traditional ones (as summarized on Table 2); then, after optimizing the design, a
169 second impact test campaign was carried out to establish the effectiveness of the supplied
170 enhancements on life-saving desks (Table 4).

171 3.3.1 *Static monotonic tests*

172 To carry out static monotonic tests a suitable setup and equipment was put on stage as shown in
173 Figure 5. The load was provided by a hydraulic Enerpac RR1010 actuator and was recorded through
174 a 100 kN load cell placed between the actuator and the devices for the load distribution. Those latter
175 consisted of (i) a H-shaped frame for the load re-distribution over the longer frame profiles placed
176 under the tabletop (Figure 5a) and (ii) a 100 mm diameter steel disk laid on the top of the desk able
177 to produce punching on the tabletop panel (Figure 5b). The displacements (both of the tabletop and
178 inner/outer frames) were only measured for the innovative desks by using HBM 100 mm inductive
179 displacement transducers (LVDTs). The location of LVDTs is explained in Figure 5c. The LVDTs
180 for tests with concentrated load were placed on the diagonal of the top of the desk, one in the centre
181 and two close to the corners, respectively, and the average tabletop's deflection was computed. For
182 the distributed load configuration, additional LVDTs were placed on the bottom of the outer frames
183 to measure their possible sliding (Figure 5c). Traditional desks' displacements weren't monitored

184 due to the expected failure mechanisms (i.e., either concentrated underneath the loading plate and/or
185 brittle).

186 Additionally, strain gauges (SGs) monitored the strain in the frame of the traditional and life-saving
187 desks. In accordance with (Figure 5d), when the applied load was concentrated, just 4 SGs were
188 applied to the profiles of the horizontal frames of life-saving desks. In accordance with (Figure 5a-
189 d), when the applied load was distributed, 16 and 32 SGs were applied to the sub-structure of
190 traditional desks and to the inner and outer frames of life-saving desks, respectively.

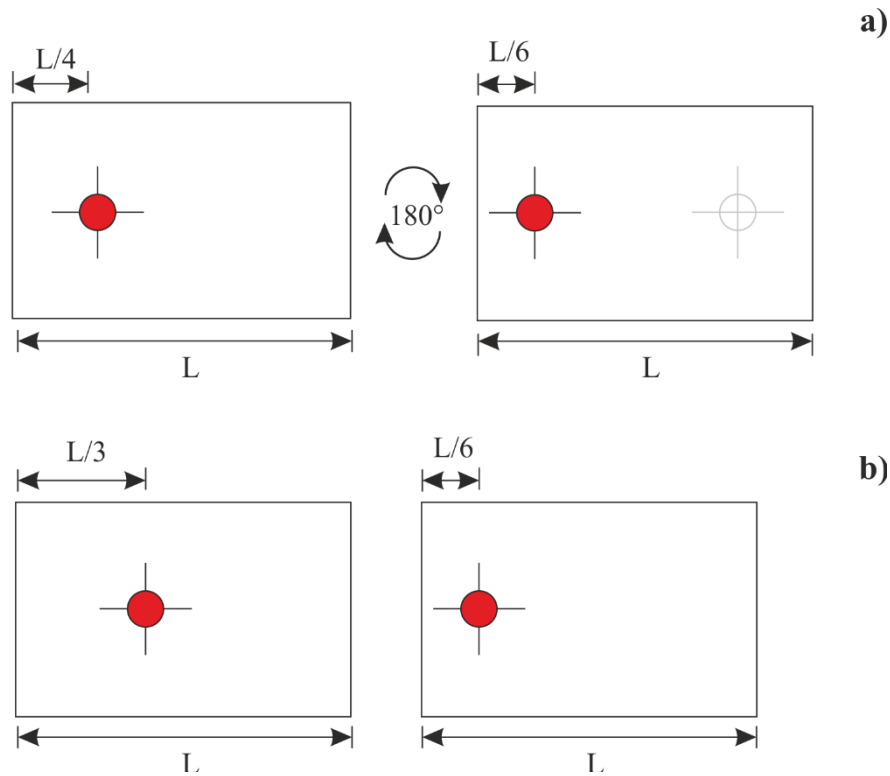


192 **Figure 5.** Monotonic tests on desks: **a)** Distributed load setup; **b)** Concentrated load setup; **c)** LVDT position; **d)** Strain-
193 gauges position for concentrated load; **e)** Strain-gauges position for distributed load

194 Concentrated load tests were all carried out with the load placed in the middle of the tabletop,
195 except for one test where the load was first applied at a distance of one fourth of the longer edge
196 from the shorter one and subsequently at one sixth of the longer edge length from the opposite
197 shorter edge (see Figure 6a).

198 In the second campaign, desks were tested as in the first one, however, for the eccentric
199 arrangements, eccentricities were modified and set equal to one third and one sixth of the longer
200 edge from the shorter edge (previously one fourth and one sixth) (see Figure 6b). The general setup
201 was the same of the previous campaign, and so were the recorded parameters. Tests were carried
202 out in accordance with Table 3, to test the potential of a new set of support (see Figure 1), not only
203 to overcome the problems highlighted with the failed specimens during the first campaign, but,
204 most importantly, with a view to the following impact tests and how these new supports would help
205 towards dissipation.

206 The tests were interrupted, as general rule, when the vertical space underneath the desk became too
207 short, to comply with the safety measures, or the vertical displacement occurred with no increasing
208 load.



209

210 **Figure 6:** Scheme of the concentrated load: **a)** First campaign; **b)** Second campaign

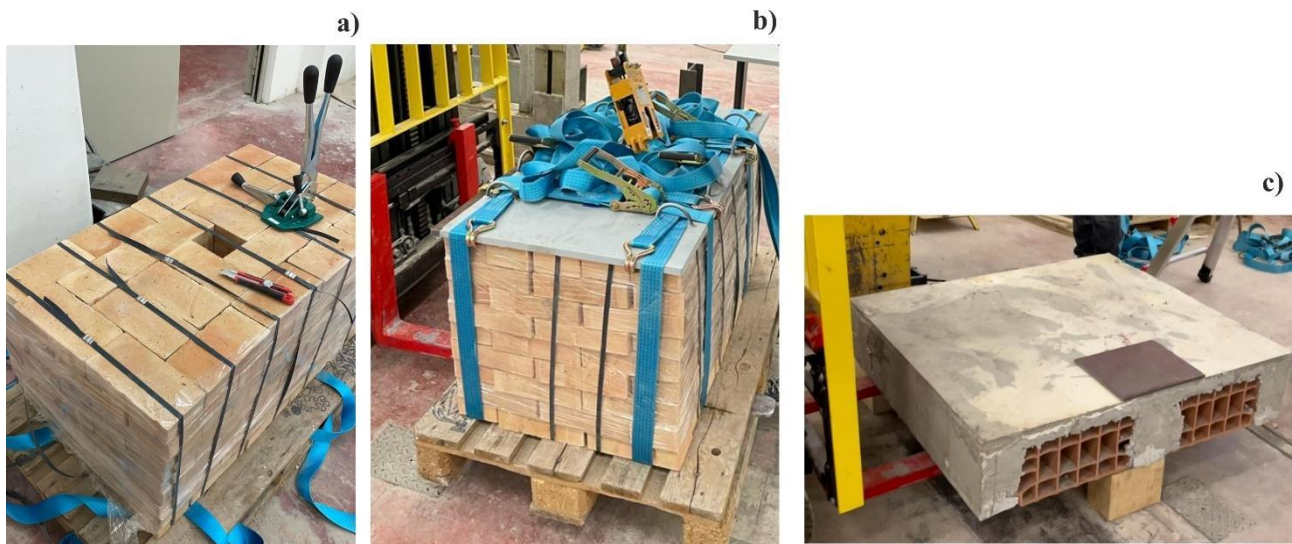
211 *3.3.2 Dynamic (impact) tests*

212 The target of the proposed life-saving desk prototypes was the safety of its user against falling
 213 objects following seismic events. Therefore, impact tests were essential to simulate the effect of a
 214 possible upper floor collapse.

215 Performing full-scale impact tests was challenging due to several reasons: they are uncommon in
 216 the field of civil engineering and differ from those made in other engineering fields that mainly test
 217 subcomponents and small-scale elements. These latter conditions required to establish a novel tests
 218 methodology. At first, a suitable height for the load release was chosen; it was 2.5 m high from the
 219 desk support surface in consideration of a realistic and common inter-storey height. To ensure an
 220 instantaneous load release, a manual, 1-Ton capacity, quick release device was employed. The
 221 amount and type of load was deeply analysed to guarantee the same features of real floors in terms
 222 of weight and stiffness. Two different scenarios were accounted for the existing floor: (i) a floor

223 built with ancient techniques as brick vaults and domes and (ii) a traditional mixed reinforced
224 concrete and hollow tiles floor.

225 The typical Italian ancient vaults are characterized by a certain flexibility, due to the thin layer of
226 mortar that keep the bricks together. In some cases, the mortar is degraded or even no longer
227 present, so, in case of collapse, incoherent parts would fall. The idea was to reproduce this
228 possibility by packing brick stacks simply overlapping and wrapping them with clamped bands and
229 plastic film stripes, rather than bonding them (Figure 7a). A steel plate was settled on the top of the
230 stack to allow its hooking and lifting, further belts were used to improve the holding.



231
232 **Figure 7:** Impact loads: a) Assembly of brick stack; b) one of the 600 kg brick stack; c) portion of mixed reinforced
233 concrete and hollow tiles floor

234 The size, height and load of the stacks were discussed to guarantee the worst impact conditions. The
235 area of the stack was assessed to be equal to the tabletop, while the height varied based on the two
236 mass amounts: 450 kg and 600 kg (Figure 7b). The effect of a traditional mixed reinforced concrete
237 and hollow tiles floor was simulated by releasing a portion of this floor having as base dimensions
238 1.0 m x 1.2 m and a height of 0.24 m. The weight of these floor portions was equal to 300 kg.
239 (Figure 7c).

240 **Table 2.** First experimental campaign: test conditions

Specimen	Types	Test type	Repetitions	Load type
V series	Proposed life-saving	Static monotonic	1	Distributed
			1	Concentrated without eccentricity
			1	Concentrated with eccentricity ($e = \frac{L}{4}$)
	Traditional		1	Concentrated with eccentricity ($e = \frac{L}{3}$)
			1	Distributed
			1	Concentrated without eccentricity
S series	Traditional	1	Concentrated without eccentricity	
	Proposed life-saving	1	Distributed	
		1	Distributed	

241

242

Table 3. Second experimental campaign: test conditions

Specimen	Types	Test type	Repetitions	Load type
V series	Proposed life-saving	Static monotonic	1	Concentrated without eccentricity

			1	Concentrated with eccentricity ($e = \frac{L}{6}$)
			3	Concentrated with eccentricity ($e = \frac{L}{3}$)
			3	Distributed
			1	600 kg
	Proposed life-saving		1	450 kg
			3	300 kg
		Impact	1	17.5 kg
	Traditional		1	450 kg
			1	300 kg
			2	36 kg
			1	Concentrated without eccentricity
S series	Proposed life-saving	Static monotonic	1	Concentrated with eccentricity ($e = \frac{L}{6}$)
			2	Concentrated with eccentricity ($e = \frac{L}{3}$)
			2	Distributed
		Impact	1	600 kg

1	450 kg
2	300 kg
1	36 kg

243

244

Table 4. Third experimental campaign: test conditions

Specimen	Types	Test type	Repetitions	Load type
	Life-saving optimized		2	
V series	Life-saving + belt		2	
	Traditional		1	
	Life-saving optimized	Impact	2	600 kg
S series	Life-saving optimized + belt		1	
	Life-saving + belt		1	

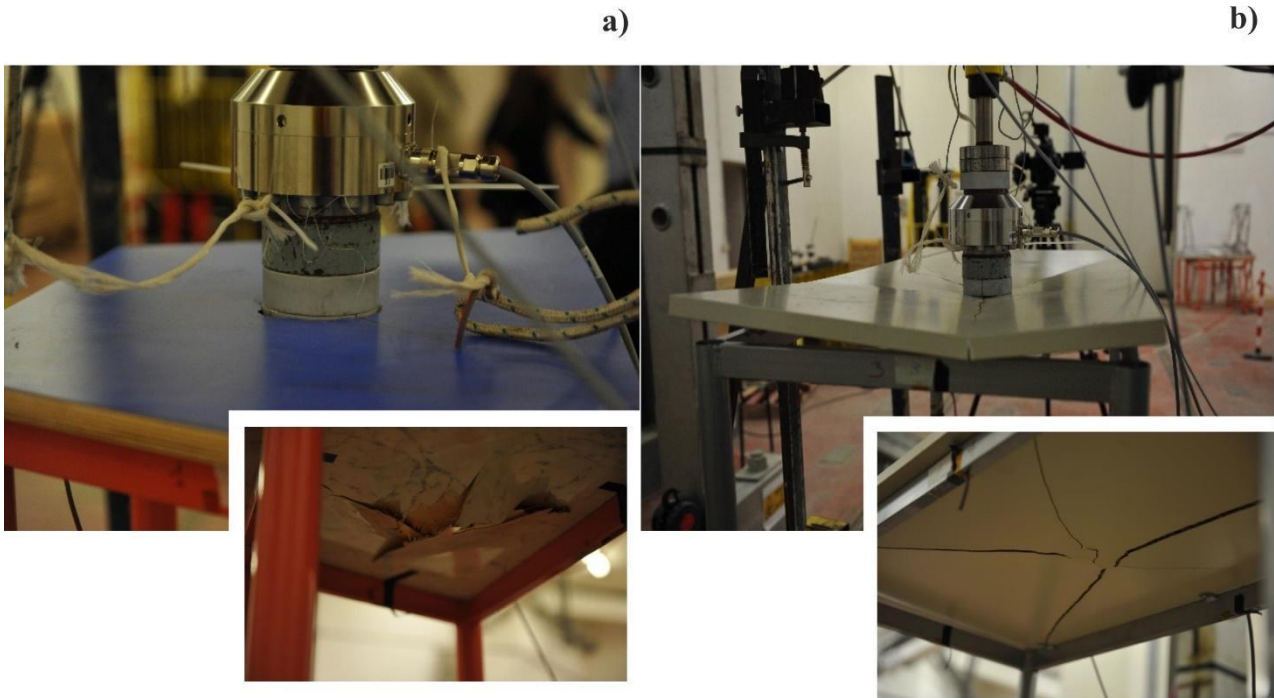
245 **3.4 Results and discussion for desks**

246 **3.4.1 First test campaign on school desks**

247 **3.4.1.1 Concentrated load**

248 For traditional desks, regardless of the usual higher capacity of the material, the multiply veneer
 249 board top fell behind the particleboards top due to the dimensions, and, consequently, supporting
 250 conditions, but, most importantly, due to the failure mechanism: the nature of the particleboards
 251 allowed it to have a concentrated failure under the loading plate, meaning the capacity were that of
 252 the material plus that provided by the friction of the failing area against the still intact surrounding

253 portion. On the other hand, the multiply board couldn't show a concentrated collapse, and the
254 resulting bearable load was massively influenced by its bending capacity (Figure 8). The
255 particleboards showed a maximum load of 24 kN, whereas the multiply board collapsed after just 7
256 kN in a very brittle manner.



257

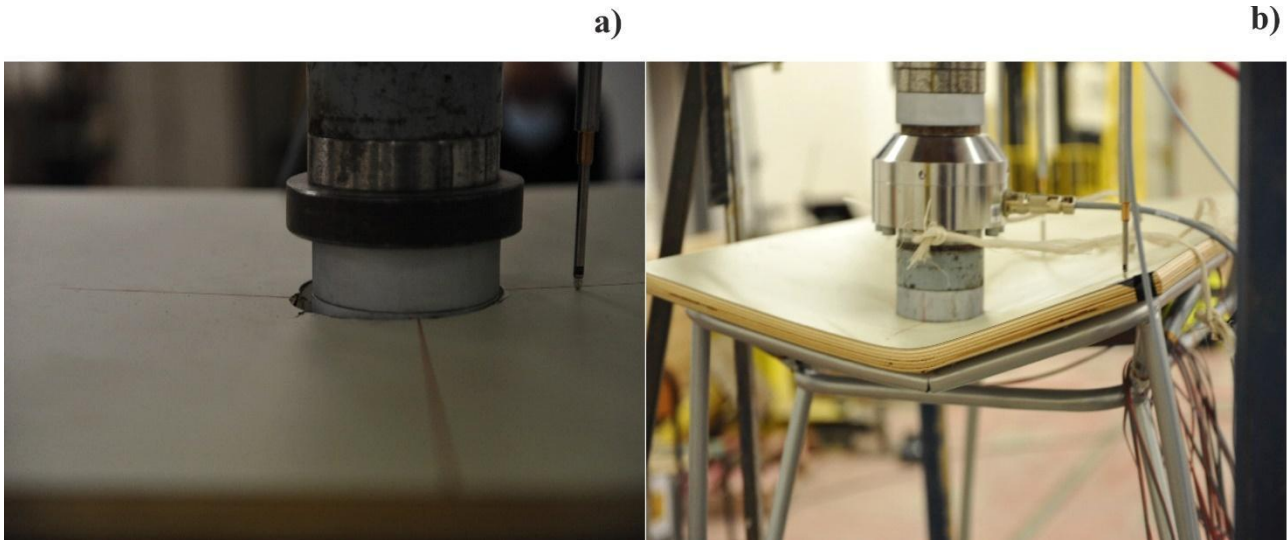
258 **Figure 8.** Traditional desks: **a)** Collapse of the PB and **a)** multiply top failure.

259 For life-saving desks, the tests highlighted how the presence of a metal sheet under the wooden
260 tabletop significantly augments strength and ductility when subject to concentrated loads if
261 compared to traditional alternatives

262 The presence of a metal sheet below the multiply board allowed the top of the innovative solutions
263 to perform in a more ductile manner, thanks to the involvement of the frame in the capacity of the
264 system against this type of load, whereas the traditional alternatives resist just with the wooden top.

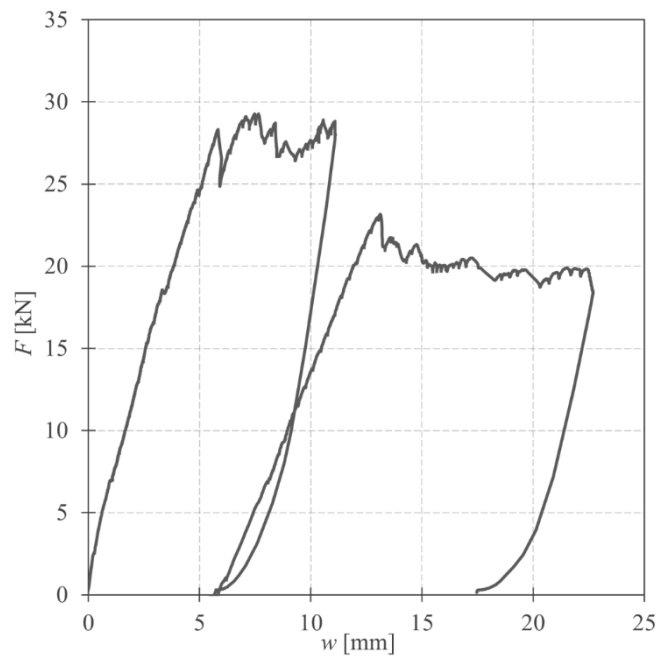
265 The centred load test showed a concentrated failure like that of the PB traditional desk, while the
266 eccentric test presented a fractured, yet ductile, collapse, more similar to the multiply board
267 traditional desk (Figure 9).

268 The first test reached a maximum load of 44 kN, while the second recorded a peak of 30 kN in the
269 first phase and 23 kN in the second and a maximum displacement at the centre of the specimen of
270 roughly 50 mm (Figure 10).



271

272 **Figure 9.** Collapse of the life-saving desks during the concentrated load test: **a)** without eccentricity and **a)** with
273 eccentricity.

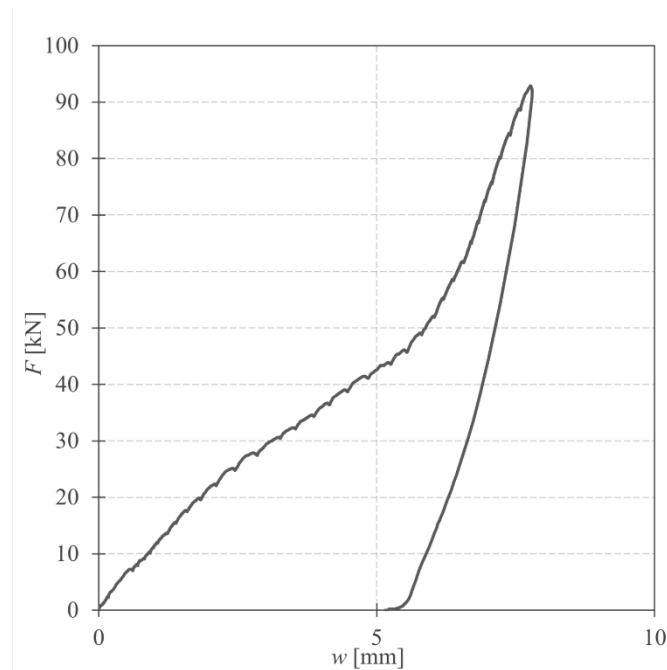


274

275 **Figure 10.** Force vs Average displacement relationship for the eccentric load tests

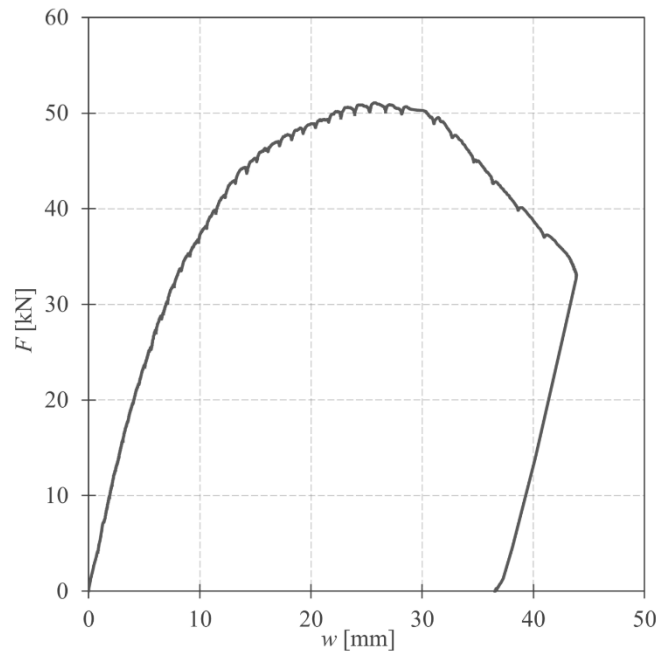
276 3.4.1.2 Distributed load tests results

277 All the traditional and life-saving desk outperformed the actuator, reaching a peak load of nearly
278 100 kN. They could have borne a higher load, but the research team agreed it is extremely unlikely,
279 in the scenarios these elements are meant to operate as safety equipment, they would be subject to
280 an accumulated mass greater than 10t. The one thing all the three tests had in common was that they
281 all showed a first milder slope in their force vs displacement curves, followed by a steeper one
282 (Figure 11). This was due to the initial collapse of the plastic supports at the base of the legs before
283 the legs could effectively touch the ground and start to be properly loaded. No significant difference
284 in terms of shape and displacement attained was spotted. For this reason, only an example curve is
285 depicted in Figure 11.



286
287 **Figure 11.** Force vs Average displacement relationship for a distributed load test on a traditional desk.

288 The fourth desk, an innovative one, suffered from a geometrical issue, resulting in an eccentricity of
289 the load in the legs due to the mutual position of the same legs and the plastic supports. Because of
290 the geometry of the new concept, one of the suppliers welded additional supports in line with the
291 legs, resulting in one of the successful tests mentioned above. The other supplier, however, used



305

306 **Figure 13.** Force vs Average displacement relationship for the collapsed life-saving desk under distributed load.

307 *3.4.2 Second test campaign on school desks*

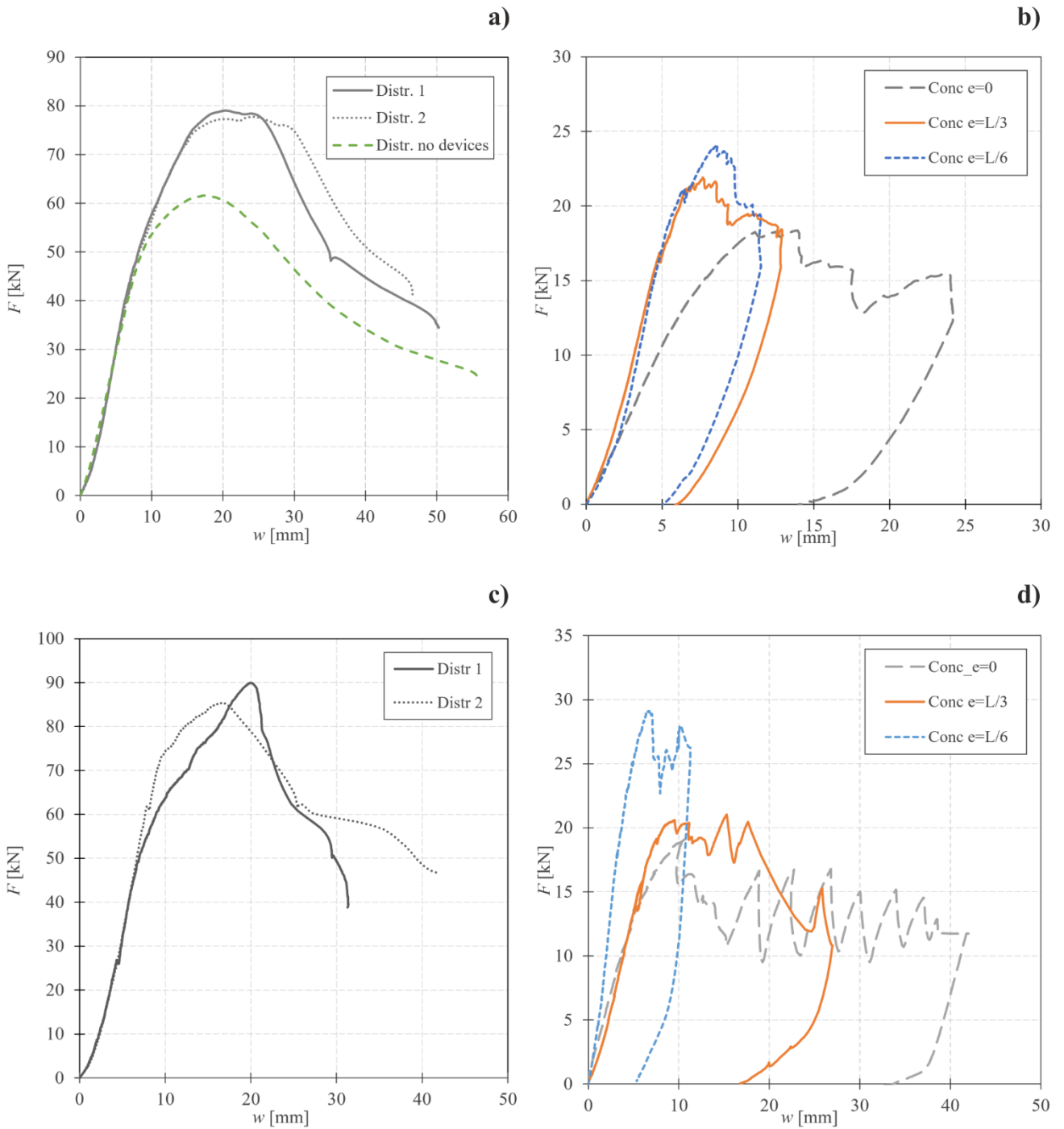
308 *3.4.2.1 Concentrated load*

309 As the load approached the frame, namely, as the point of application moved from the centre to the
 310 edge, the specimens showed a higher capacity, yet a lower ductility, as can be seen in Figure 14b
 311 and d. The results for the two series are reported separately for clearness: Figure 14a and b depict
 312 the V-series, whilst Figure 14c and d the S-series. No difference in the overall behaviour of the
 313 desks was observed with respect to the first campaign, as the mode of failure was compatible with
 314 those encountered previously.

315 *3.4.2.2 Distributed load tests results*

316 The results of the tests are depicted in Figure 14a-c. The proposed dissipative foot, shown in Figure
 317 15 at the end of the loading test, even if determining a lower capacity of the system, generated a
 318 more ductile response of all the specimens. The mode of failure detected was the same as that of the
 319 previously failed specimen, but, in this case, being the supports not perfectly identical, they crashed

320 differently, and once the first was flattened, a different distribution of load started in the legs,
 321 causing the same, yet more controlled, rotational movement seen in the first campaign.



322
 323 **Figure 14.** Force vs Average displacement relationship for distributed load tests – second campaign: **a)** Distributed
 324 loads V-Series, **b)** Concentrated loads V-Series, **c)** Distributed loads S-Series, **d)** Concentrated loads S-series

325



326

327 **Figure 15.** Proposed dissipative foot collapsed after the loading test

328 3.4.3 *Dynamic (impact) test results*

329 The reliability of desks as a safe shelter in case of earthquake was assessed also via impact tests.

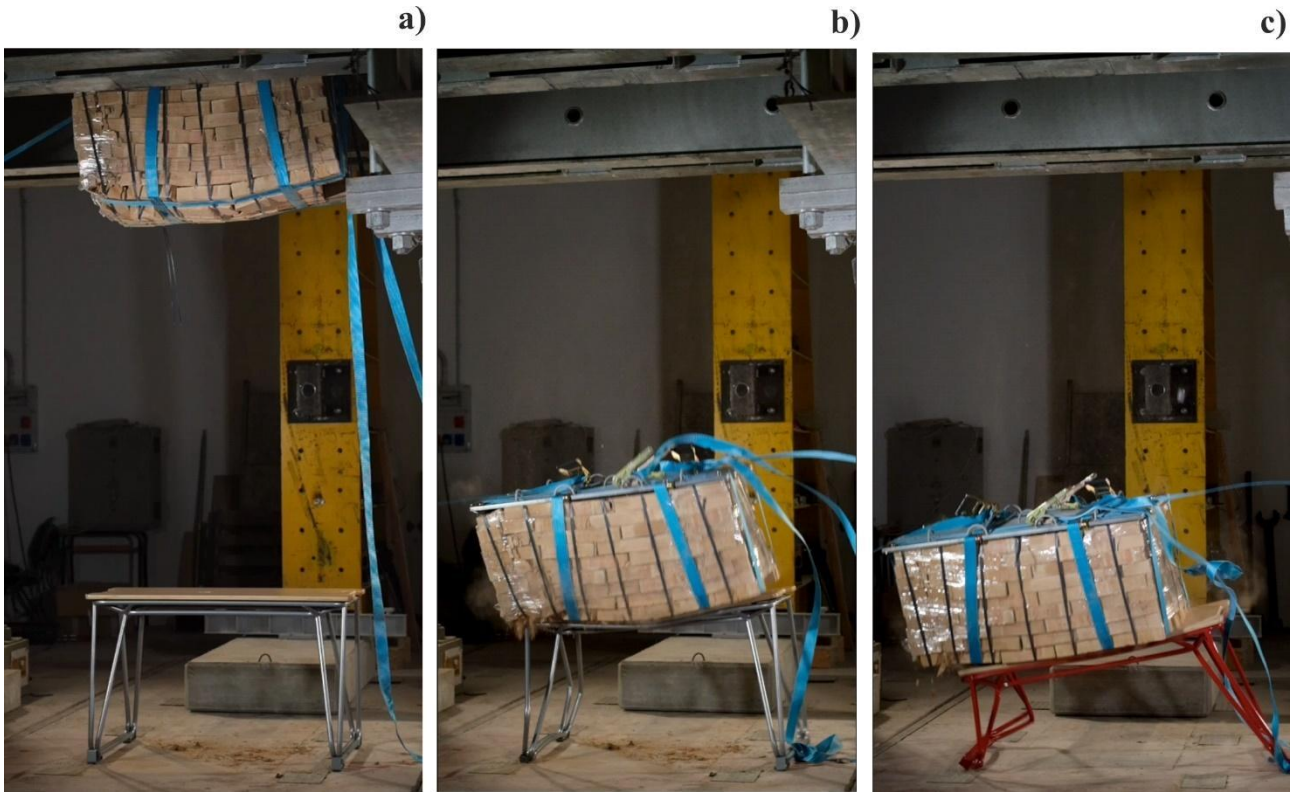
330 The first tests were carried out with brick stacks weighting 600 kg. Both for the V and S prototype,

331 the outer vertical frames bent outwardly in the lower part with a ductile mechanism; in particular,

332 the little mass eccentricity caused a more severe outer vertical frames damage for the V one (Figure

333 16).

334



335 **Figure 16.** Impact test performed with a brick stack of 600 kg: **a)** test setup prior to release; **b)** impact moment on S
336 prototype; **c)** impact moment on V prototype

337 Tests carried out with brick stacks of 450 kg gave good evidence; although the bending mechanism
338 was still observed, the frames didn't collapse, and the tabletop was intact, ensuring the life-saving
339 function (Figure 17a-b). Tests highlighted, in both cases, an excessive relative horizontal sliding of
340 outer vertical frames at the floor level. This condition was accounted and fixed in the second
341 version of the prototypes by suitably connecting them to the inner ones.

a)



b)



342

343 **Figure 17.** Impact test performed with a brick stack of 450 kg: **a)** impact moment on V prototype; **b)** impact moment on
344 S prototype

345 Other tests were carried out by releasing the 300 kg floor portions. In this case, the most remarkable
346 result for life-saving desks was the bending of the outer vertical frames; neither the horizontal
347 frames nor the tabletop were damaged (Figure 18). On the other hand, the traditional desk was
348 severely damaged, with one leg crashed and compromised stability.



349

350 **Figure 18.** Impact test performed with a floor portion of 300 kg: **a)** test setup prior to release; **b)** impact moment on S
 351 prototype; **c)** after the impact moment on S prototype; **d)** after the impact moment on V prototype; **e)** after the impact
 352 moment on traditional desk

353 Finally, further tests were carried out with reduced loads (17.5 and 36 kg) with the aim to test the
 354 tabletops breakout strength in case of collapse of non-structural ceiling elements (i.e., lights, false
 355 ceiling portion or projectors). In this case, small cubic packs of bricks were realized and released.
 356 As it is evident from Figure 19, the effect of 36 kg load release on traditional and life-saving desk
 357 was the opposite: the traditional tabletop experienced a complete breach of the timber panel and the

358 separation between the top and the steel frame (Figure 19a-b); the life-saving desk was able to resist
359 by assuring a dissipation of energy through the dissipative feet (Figure 19c-d).



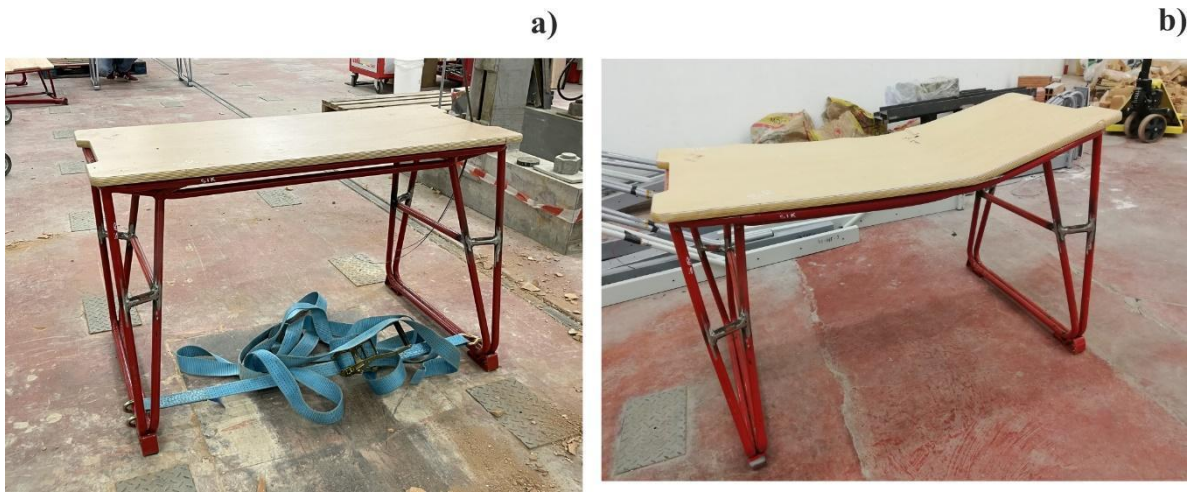
360

361 **Figure 19.** Impact test performed with a floor portion of 36 kg: **a)** traditional desk tabletop breach; **b)** traditional desk
362 tabletop-frame separation; **c)** impact on the life-saving desk; **d)** with energy dissipation; **e)** and overall bouncing.

363 3.4.4 Third test campaign on school desks

364 The third test campaign was performed after updating the prototypes with suitable reinforcements
365 specifically added to fix the weaknesses highlighted in the previous test campaigns (as described in
366 the previous section). Thereafter, only the most critical tests with the heavier 600 kg weight were
367 repeated. As a results for the optimized specimens of both the series, it was highlighted that the
368 bending of the outer vertical frame was prevented due to the welded additional profiles;
369 nevertheless, the tensile action causing base sliding was still present. To avoid this latter issue, as a
370 quick and effective method, a ratchet belt was tightened between the two side frames (Figure 20a).

371 As a result, during the impact, no slip was recorded. This solution was suitably implemented in the
372 final desk prototypes as an additional welded tube-shaped tie-rod.



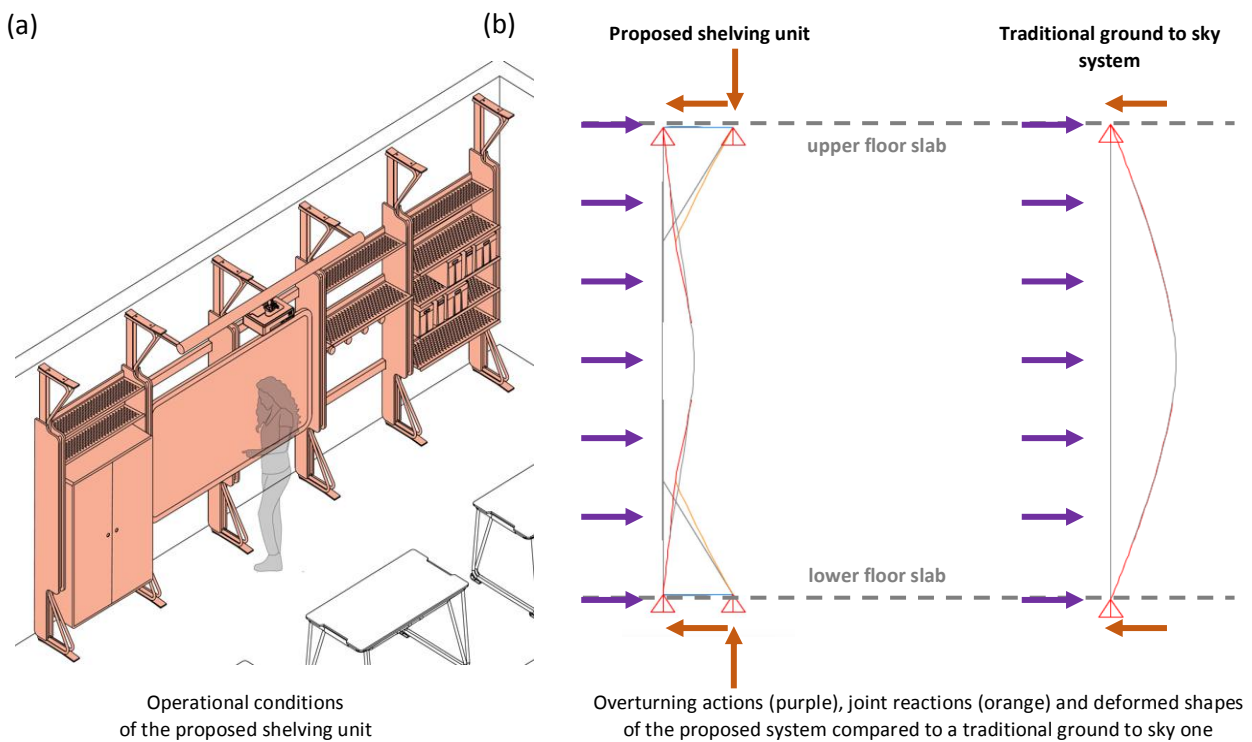
373
374 **Figure 20.** Impact test performed with a floor portion of 600 kg: **a)** test setup with ratchet belt; **b)** the
375 prototype after the impact

376 **4 Self-supporting shelving unit**

377 **4.1 Structural conceptualization**

378 Standard shelving units are installed next to a wall and fixed to it through mechanical fasteners.
379 Alternatively, they can be freestanding units adjustable in height and secured to the floor and
380 ceiling. Existing research, including studies [19-23] and international standards such as FEMA E-74
381 [24], California [25], and Japanese school guidelines [26], primarily focus on securing classic
382 bookshelves to classroom walls for seismic mitigation. However, beyond this basic measure,
383 dedicated research on the seismic performance of these structures is limited. A significant issue
384 with these solutions is that if partition walls don't meet seismic standards, the anchored shelving
385 unit undergoes the same wall's damage or could even be a worsening factor. Similarly, shelving
386 units anchored solely to the floor and ceiling, without additional bracing, are at risk of collapsing
387 during an earthquake due to the potential overturning of adjacent partition walls.

388 The proposed self-supporting shelving unit (Figure 21) addresses the limitations of existing designs
 389 by serving both as a functional storage solution and a safety device. In normal conditions, it works
 390 as a bookshelf hosting interactive whiteboards, teaching materials, and audiovisual equipment
 391 (Figure 21a). However, in the event of an earthquake (Figure 21b), the unit is designed to protect
 392 nearby people by (i) preventing the collapse of the adjacent partition wall and (ii) shielding them
 393 from falling debris. More in detail, Figure 21b compares the behaviour and deformed shape of the
 394 proposed self-supporting shelving unit (left in Figure 21b) to the one of a traditional sky to ground
 395 one (right in Figure 21b) in case of a seismic event. The purple arrows represent the earthquake
 396 action, while the orange arrows represent the opposing reactions of the two shelving units. The
 397 proposed system is significantly stiffer than the traditional one thanks to the presence of the upper
 398 and lower triangular elements that reduce the free span of deflection of the shelving unit. Moreover,
 399 the stiffening triangular profiles increase the axial compressive load under horizontal deflection
 400 improving the horizontal friction resistance to horizontal loads.



401

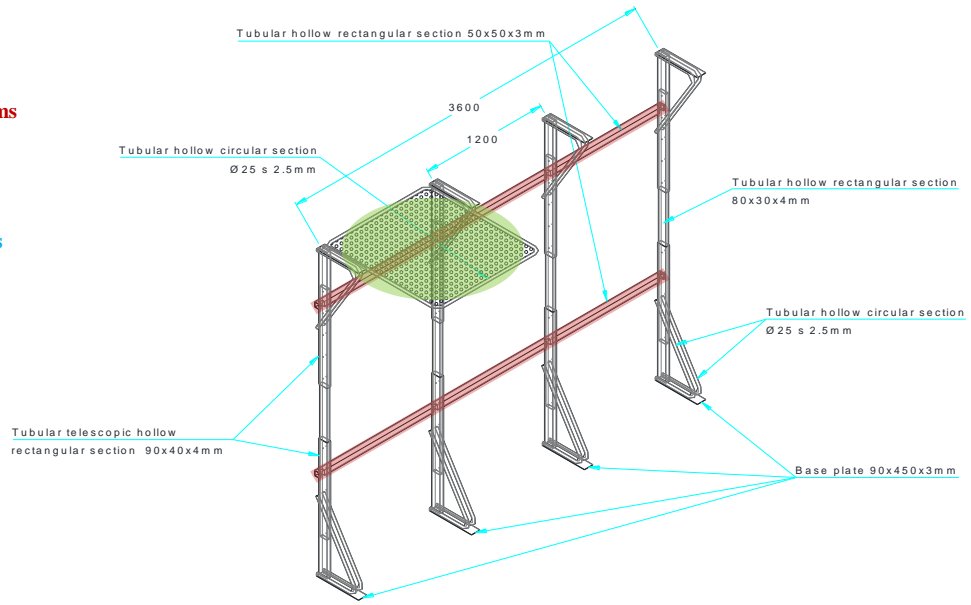
402 **Figure 21.** Working conditions of the proposed shelving unit: (a) operational ones; (b) in case of earthquake

403 Figure 22 portrays the structural layout of the proposed self-supporting shelving unit whose
404 uprights are the core elements. Each upright is composed of three elements, a central rectangular
405 hollow profile, sized to work mainly for bending and axial forces, and two symmetric stiffening
406 triangular profiles, subjected to axial force and hosting the central profile. The triangular profiles
407 can be slid over the central one to adjust the height, creating a versatile floor-to-ceiling structure
408 that can fit heights spanning from 2.70 m up to 3.00 m. Once reached the desired height, the
409 triangular profiles are secured to the central profile using self-tapping metal screws. This
410 configuration reduces the free length of deflection of the central profile, empowering
411 simultaneously the performance of top and bottom restraints thanks to the compressive action
412 developed, whilst also simplifying the carriage and installation procedures. The shelving unit will
413 only fail if its connection to the floors is compromised or if the structural capacity of its members is
414 overcome. In addition, a prestress force is applied to the struts to increase the efficiency of the
415 restraints (higher friction resistance) and to maximize the efficacy of a layer of elastomeric material
416 located at the interface between the metal support plates, installed at each end of the uprights, and
417 the floors. The elastomeric layers are meant to create a continuous contact surface and to increase
418 the resistance against sliding. Each upright is connected to the successive one thanks to crossbeams,
419 for an overall length of the shelving unit of 3.60 m.

420 Each of the three modules composing the shelving unit spans 1.20 m and it can accommodate a
421 protective top panel, allowing to achieve the second objective of the life-saving shelving unit, that is
422 providing protection against falling debris for students or people that cannot use school desks as a
423 shelter. To this aim, the length of 1.20 m grants enough space to protect a person in a wheelchair
424 plus an assistant. It is also worth to observe that the proposed system is realized with prefabricated
425 elements, thus, simplifying its production and availability.

Crossbeams

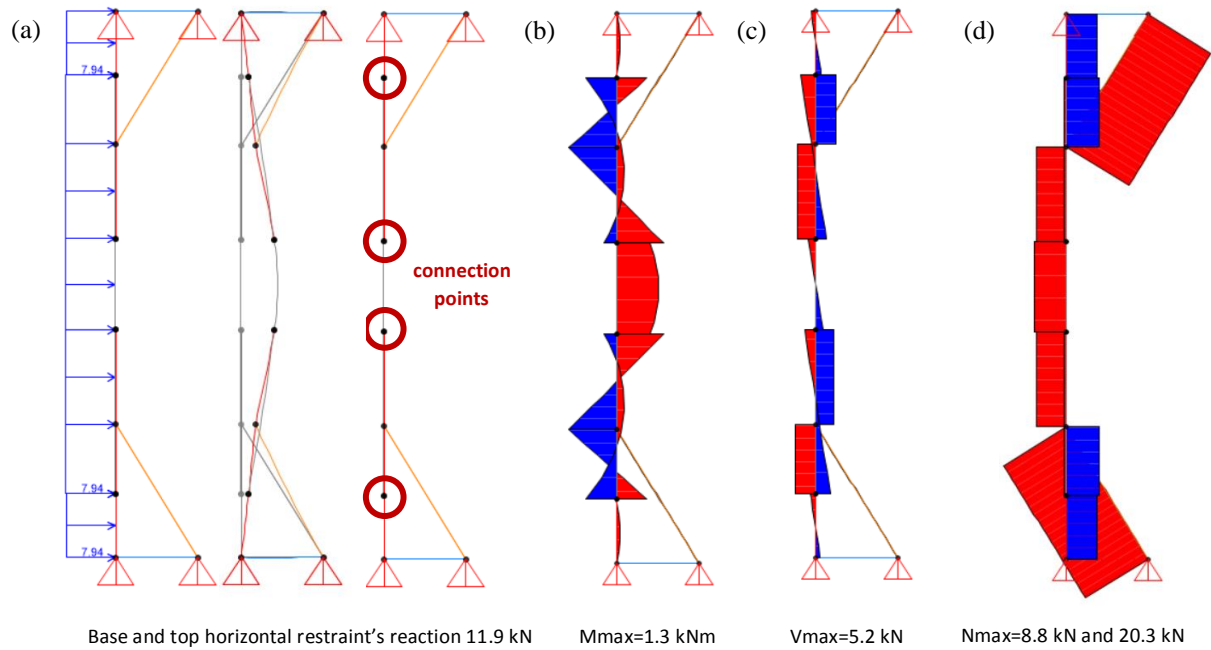
Uprights



427 **Figure 22.** Layout of the proposed self-supporting shelving unit

428 4.2 Prototypes

429 The shelving unit was designed to sustain the overturning action produced by a typical infill
430 partition wall, used within reinforced concrete (RC) frame structures realized between 1960-1990,
431 consisting of a 2 cm thick layer of plaster that covers each of the two faces of 8 cm thick hollow
432 bricks. For the estimation of both the dimension and the maximum acceleration suffered by the
433 infill wall, a real school in the city of Ascoli Piceno, Italy, was taken as case study [27]. With
434 reference to the infills under consideration (length 7.60 m, height 3.0 m), a shelving unit was
435 dimensioned having a total length of 3.60 m and a depth of 0.45 m, encompassing 4 uprights able to
436 span a height between 2.70 m and 3.0 m and 2 crossbeams able to distribute among the uprights the
437 overturning action of the partition wall (Figure 22). The seismic action, representative of the
438 demand for the dimensioning and check of infills partition towards overturning action and
439 consequently to the shelving unit, was defined according to Italian Building Standards [28] $F_a = S_a$
440 W_a/q_a where $S_a = 1.96 g$ is the maximum acceleration experienced by the infill partition during an
441 earthquake having a probability of occurrence of 10% in 50 years (i.e., a return period of 475
442 years); $W_a = 36 kN$ is the weight of the non-structural component and $q_a = 1$ is the behaviour factor.
443 It is useful to specify that the maximum acceleration S_a was defined in agreement with a simplified
444 expression valid for RC frame buildings, as suggested by the instructions for the applications of
445 Italian Building Standards [28], while the q_a was assumed equal to one, instead of two as suggested
446 for infills and partition walls, for safety reasons and to free the design action from a specific infill
447 partition. Accordingly, the seismic design action to be considered for the proposed self-supporting
448 shelving unit results in $F_a = 71.5 kN$, i.e., each of the two internal uprights are designed to carry 1/3
449 (23.8 kN) of such force according to their influence areas.



450
 451 **Figure 23** FEM model of the single telescopic upright: **a)** applied load, deformed shape and number of connection
 452 points among profiles; **b)** bending action; **c)** shear action; **d)** axial action

453 Two Finite Element Models (FEMs) for a single stud related to the maximum height of 3.0 m,
 454 loaded with one third of the design action F_a distributed over the stud's height, were implemented in
 455 the SAP2000 software. The models differ for the number of connection points between the central
 456 tubular profile and the two telescopic stiffening profiles. Figure 23 shows the one that provided the
 457 highest stresses that were used for the dimensioning of the cross sections of the elements composing
 458 a single stud. Once known the stresses on the structural elements, their dimensions were defined as
 459 follows: central profile 80×30×4 mm, telescopic tubular profiles 90×40×4 mm, circular stiffening
 460 profiles with diameter 25 mm and thickness 2.5 mm, base and top plates 90×450×3 mm.

461 4.3 Prototyping and tests

462 The experimental campaign was carried out at the laboratory of the Department of Civil,
 463 Construction-Architectural and Environmental Engineering (DICEAA) of the University of
 464 L'Aquila. The self-supporting shelving units were tested to achieve their maximum horizontal load-
 465 bearing features by performing static cyclic tests with real boundary constrains conditions.

466 The test methods were specifically designed for the tested elements. However, given the
467 significance of research on non-structural components during seismic events, a technical guideline
468 was recently proposed, providing standardized testing protocols, facilitating easy replication by
469 researchers and companies, such as for qualification purposes [29].

470 4.3.1 Tests methods

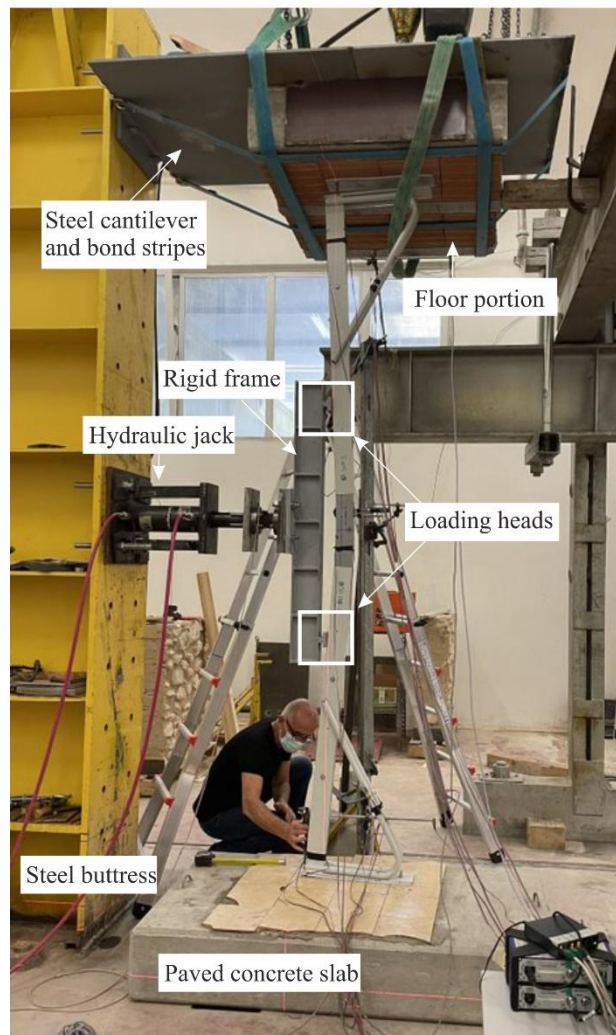
471 The two industrial partners involved in the project of the life-saving furniture system realized four
472 uprights each; neither of them used the cross-sections of the structural members designed because
473 of availability. The result are two versions of the shelving unit, one with heavier profiles and one
474 with lighter profiles, which represent a sort of Upper Bound Design Properties (UBDPs) and Lower
475 Bound Design Properties (LBDPs). However, in both cases the triangular profiles were realized
476 with circular hollow sections characterized by slightly lower thicknesses. Therefore, the tests
477 performed on these prototypes provided the opportunity to evaluate the influence of the different
478 stiffness on the activation of the inclined leg static scheme expected, on the ultimate capacity of the
479 members and on the efficiency of the different restraints tested. These latter spans from double-
480 sided adhesive tape to mechanical fasteners for concrete surfaces.

481 The cyclic experimental tests performed aims to shed light on: (i) the efficiency of the different
482 solutions for the base restraints in contrasting the sliding; (ii) the efficiency of the top restraint with
483 different values of prestress force, when the upright is installed below a concrete joist of the floor or
484 below the hollow tiles element of the traditional floor; (iii) the effective activation of the inclined
485 leg mechanism and the characterisation of the element belonging to the telescopic studs that leads to
486 the failure of the system.

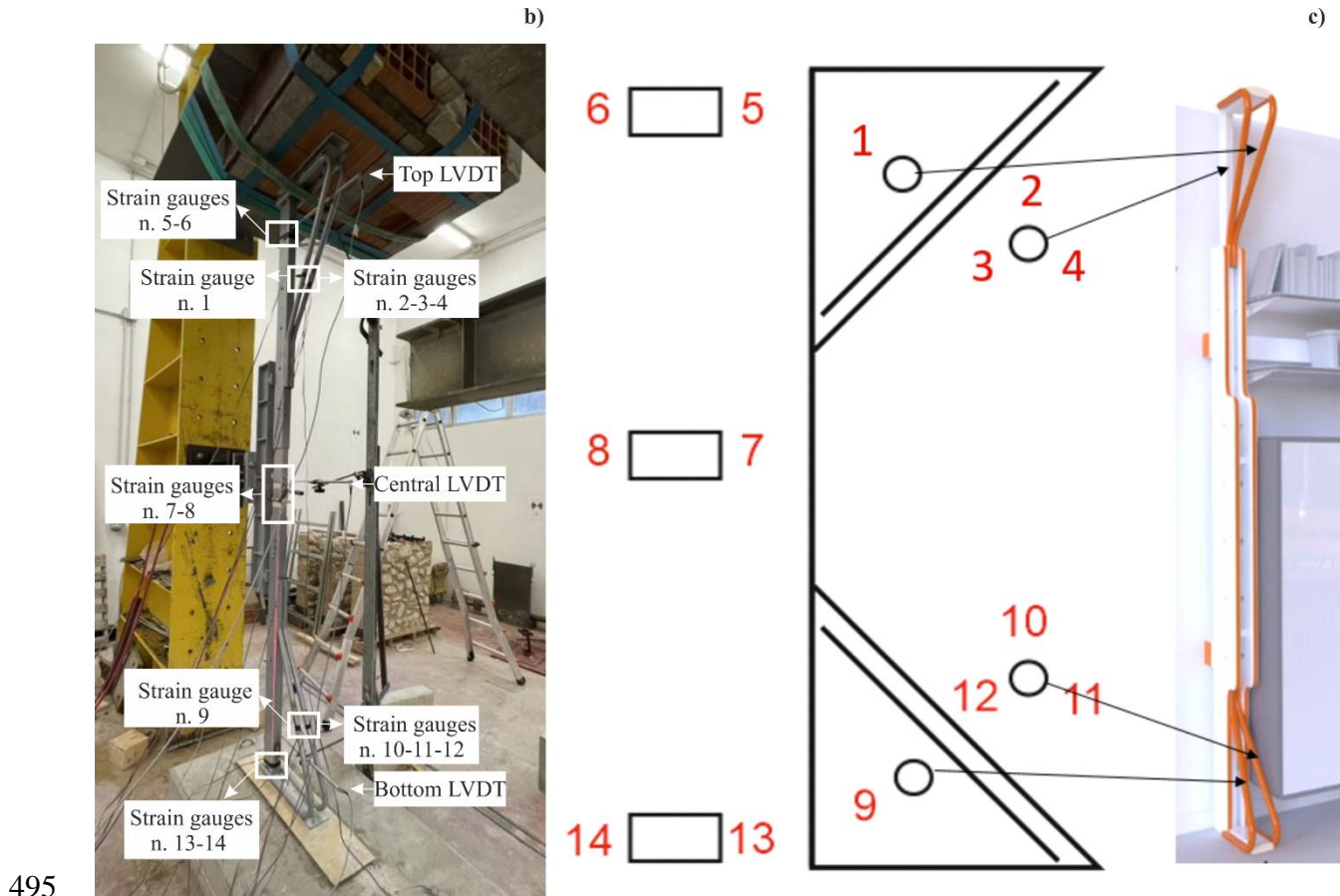
487 The test setup (Figure 24a) and boundary conditions were arranged to suitably reproduce the worst
488 real working conditions of the self-supporting shelving unit in case of seismic events; this consists
489 of the pushing effect of a typical infill partition on the telescopic uprights, which may cause its

490 overturning. The stud was symmetrically loaded at two points $1/3$ of the total length apart (Figure
491 24b-c). The load was applied by a double effect, 300 kN hydraulic jack which spreads the load via a
492 rigid frame fixed sideways the piston on the loading heads. The whole system was secured to a steel
493 buttress by a bolted connection.

a)



494

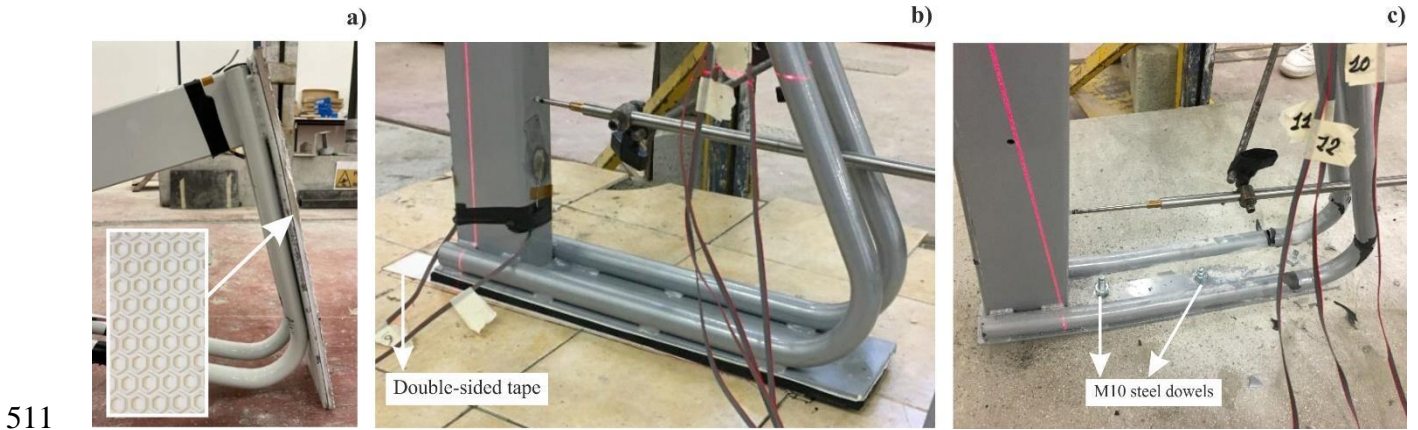


495
 496 **Figure 24:** Static test performed on the LBDPs prototype: **a)** test setup; **b)** test instruments; **c)** strain gauge position

497 The upper and lower setup boundary elements were realistically reproduced by manufacturing,
 498 respectively, a reinforced concrete paved slab and some traditional reinforced concrete joist and
 499 hollow tiles mixed floor portions. This latter was secured to a steel cantilever through high
 500 resistance bond stripes; moreover, additional support was given by the overhead crane vertical
 501 pulling action. This arrangement was settled to avoid undesired vertical compressive load on the
 502 upright. Instruments, such as LVDTs and SGs, were placed on the self-supporting shelving unit
 503 components (Figure 24) to measure the horizontal displacements as well the strains evolution in
 504 some specific points. The loading cell was suitably placed between the jack and the rigid beam that
 505 distribute the load.

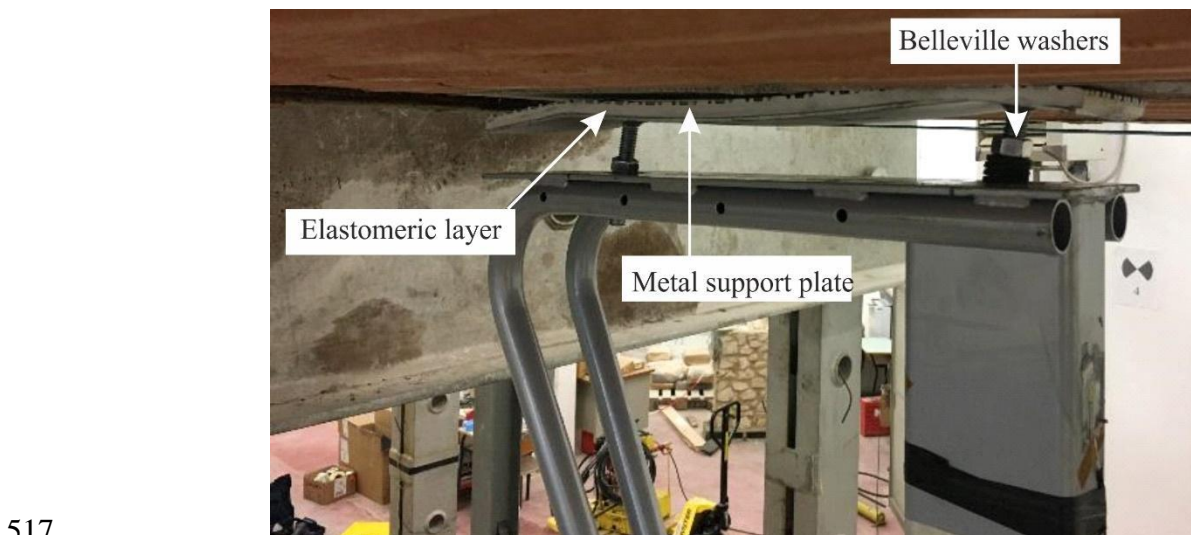
506 Both versions of the shelving unit were tested under different boundary configurations with the aim
 507 of gradually increasing the system's bearing capacity. A layer of elastomeric material accomplished

508 the base contact between the concrete slab and the metal plate (Figure 25a). Setting this as reference
509 configuration, the base contact was successively increased by adding (i) three stripes of double-
510 sided tape (Figure 25b) and (ii) steel dowels (Figure 25c).



512 **Figure 25:** Base restraint: a) Elastomeric layer; b) Elastomeric layer + double-sided tape; c) M10 steel dowels

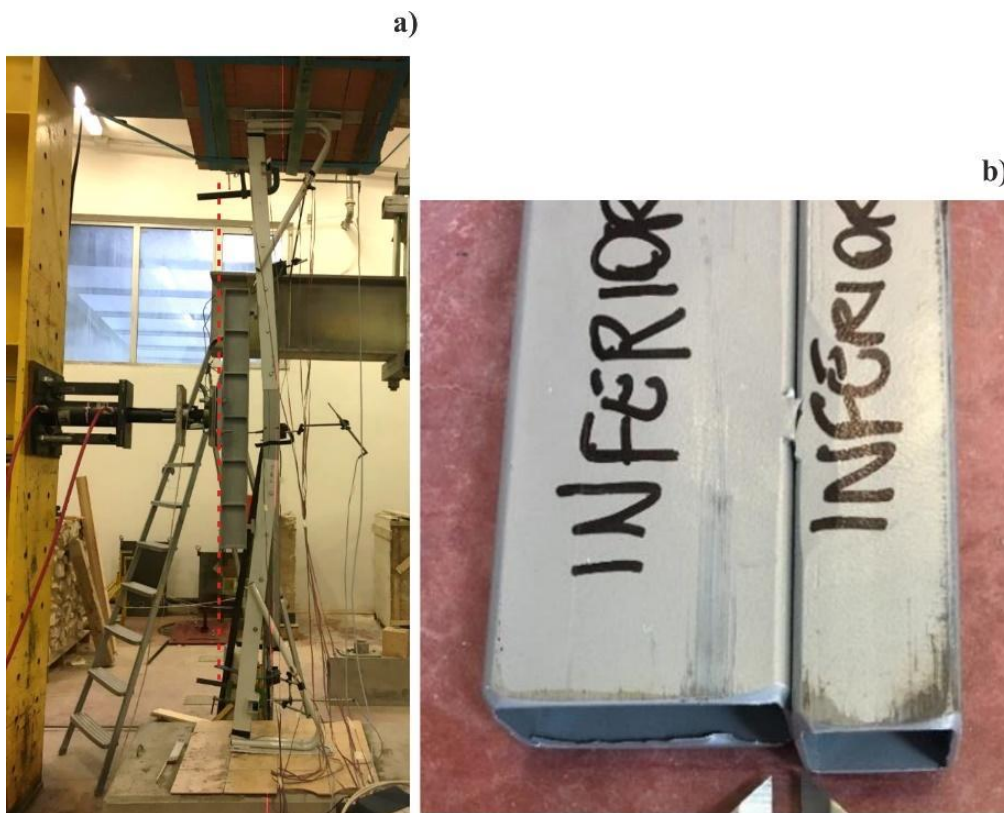
513 A layer of elastomeric material realized the contact between the ceiling floor and the metal support
514 plates. Additionally, Belleville washers were provided to apply a vertical prestress force (Figure
515 26). Finally, the stud's strength was tested by removing the metal support plate and employing only
516 steel dowels to join both the base with the concrete slab and the ceiling floor with the upper plate.



518 **Figure 26:** Metal support plate and Belleville washers

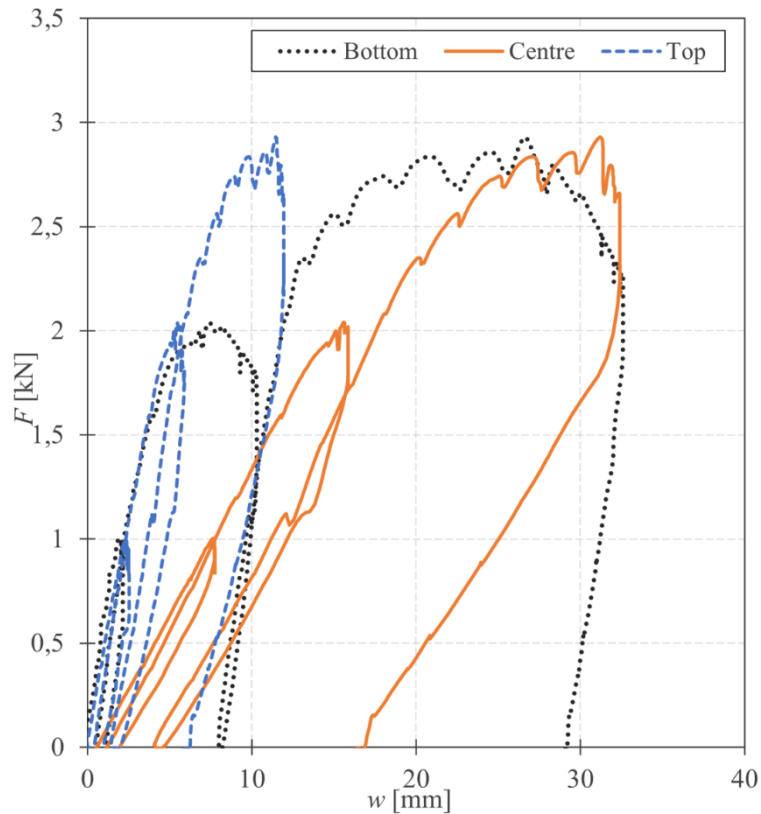
519 **4.4 Results and discussion**

520 The prototype describing the LBDPs of the telescopic uprights was first tested under the reference
521 configuration conditions with the upper metal support plate placed under the concrete joist of the
522 ceiling floor and 4 kN prestress force applied by the Belleville washers clamping. The resulted
523 restraints activation was evident from the consequent upright arched deformation shape (Figure
524 27a). The test ended when the welding joints between the two upright profiles started to collapse
525 (Figure 27b). The recorded force was 6.5 kN.



527 **Figure 27.** First test evidences: **a)** Arched deformation shape; **b)** Detail of weld joint collapse.

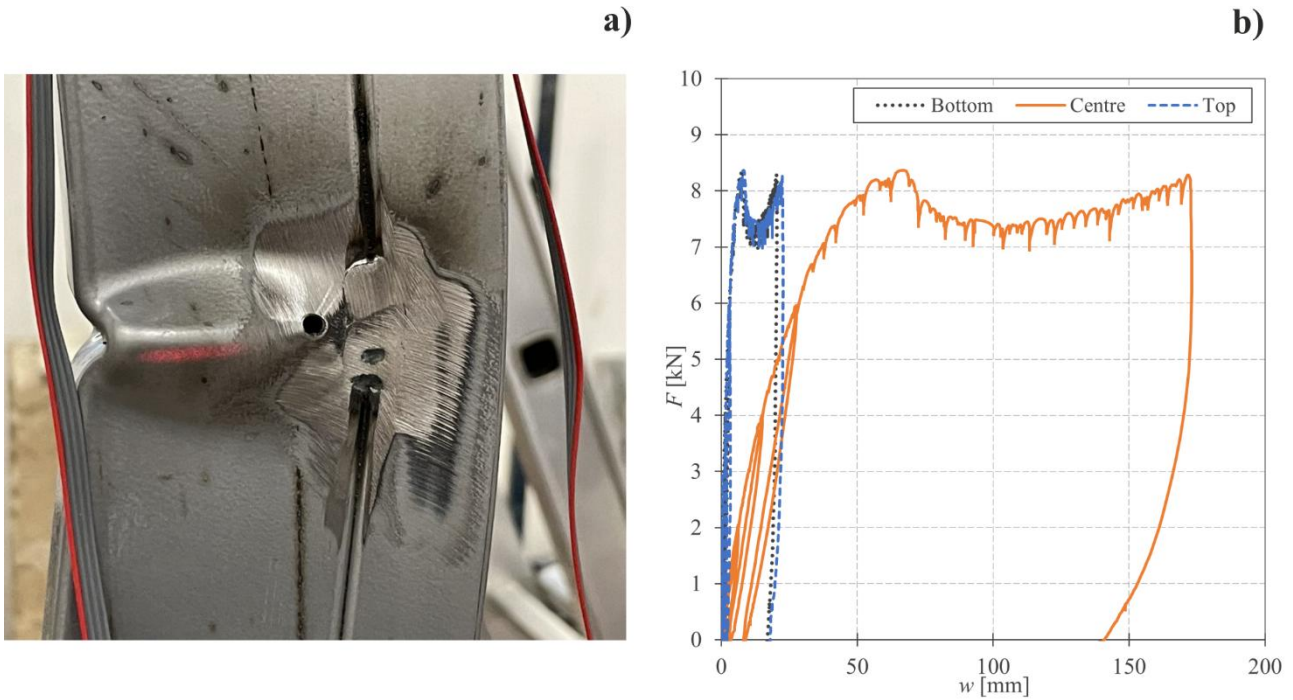
528 The following two tests were carried out by putting the upper metal support plate under the hollow
529 tiles of the ceiling floor. The washers' prestress force was, as a precaution, reduced to 2 kN in the
530 first test and then brought back to 4 kN in the second one. In both cases, the activation of base
531 sliding mechanisms caused test interruption at an applied force level of 3 kN (Figure 28).



532

533 **Figure 28.** Force-displacement plot that highlights the base sliding

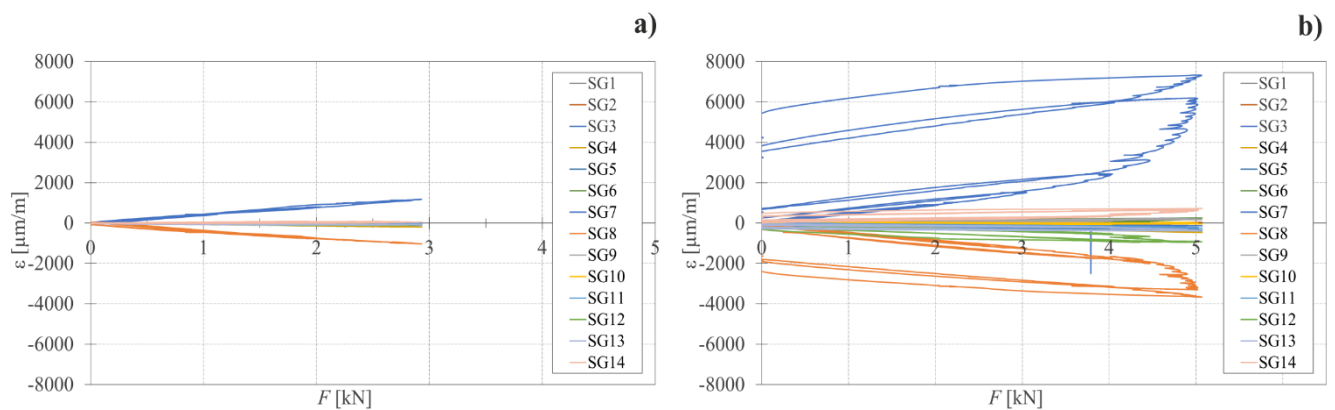
534 The fourth test was carried out by putting two additional M10 dowels as base connection to prevent
 535 the plate sliding; the washers' prestress force was 2 kN. By adopting this solution, the base plate
 536 was suitably fixed, therefore, the upright arched deformation shape was observed. Despite the
 537 prestress level being kept low, the test ended due to the hollow tile breach. The recorded applied
 538 force was equal to 5 kN. The last test was done to investigate the upright strength; therefore, the
 539 upper and lower plates were fixed to the concrete joist and to the base plate, respectively, by three
 540 M10 dowels each. The expected stud arched deformation was observed and a higher maximum
 541 horizontal force equal to 8.5 kN was recorded. The most relevant damage involved the inclined
 542 hollow circular profiles and the local buckling of the upright hollow box profile (Figure 29).



543

544 **Figure 29.** Strength test with dowels: **a)** Local buckling of upright profiles; **b)** Force-displacement plot that
545 highlight the restraint activation

546 In Figure 30, the comparison of strain-force in test three, where the base sliding occurred, and test
547 five, where the presence of dowels avoided this phenomenon, is provided. The mechanical fasteners
548 allowed the arch deformation with evident upright plasticization in the centre line points, as
549 recorded by SG 7 and 8.

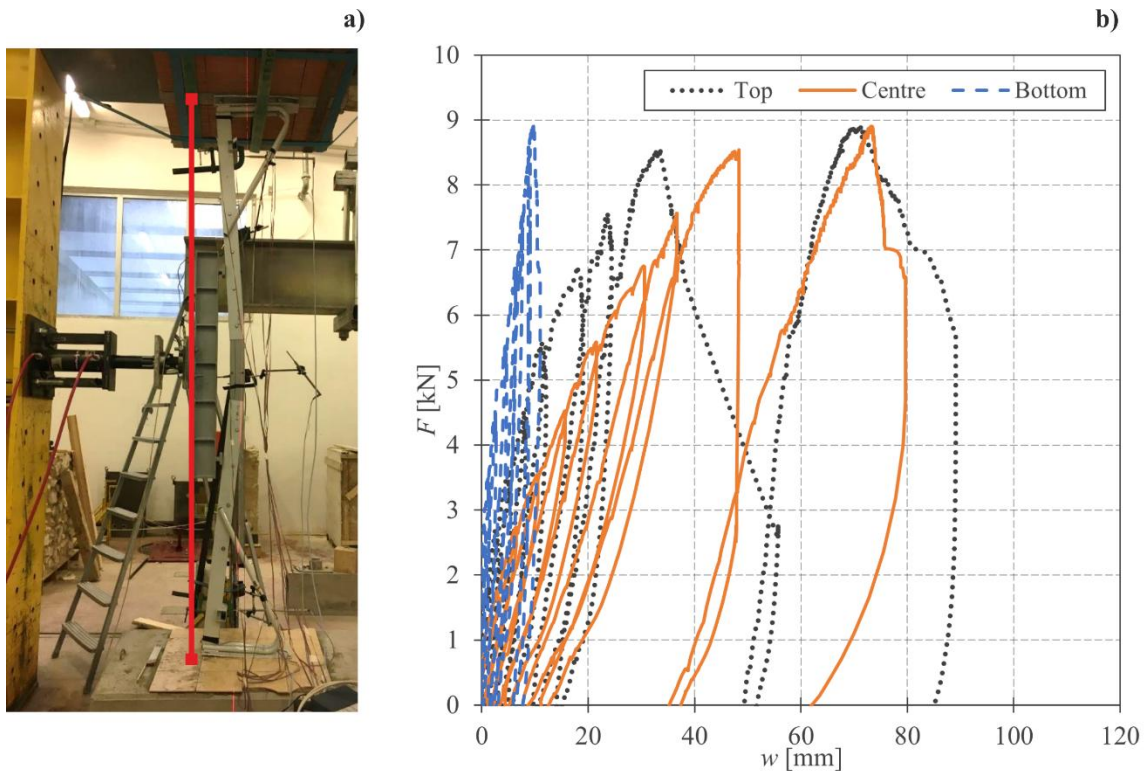


550

551 **Figure 30.** Strain-gauges results: **a)** Test three with base sliding; **b)** Test five with upright plasticization

552 The prototype describing the UBDPs of the telescopic uprights was tested too. As before, the first
553 two tests were carried on under the reference configuration, with the upper metal support plate

554 placed under the concrete joist of the ceiling floor and prestress forces of 4 kN and 8 kN,
 555 respectively. The same results were achieved, consisting in a base sliding for a horizontal load level
 556 of 3.0 kN. The washers' prestress force was maintained equal to 8 kN also in the next two tests. The
 557 third test was performed by adding three double-sided tape strips at the base, so to increase the
 558 bonding and to avoid the sliding. Beside the maximum force level doubled in the latter tests, sliding
 559 mechanism kept on developing. For the fourth test, the base connection was realized by adding two
 560 M10 dowels. As highlighted for the LBDPs, the use of steel connectors generated a fixed restraint at
 561 the base, therefore, the upright arched deformation shape was observed. After the application of a
 562 horizontal force of 8.5 kN, the upper metal support plate slid, and the test stopped (Figure 31). The
 563 static scheme changed from simply supported beam to cantilever due to the weakening of the upper
 564 restraint.

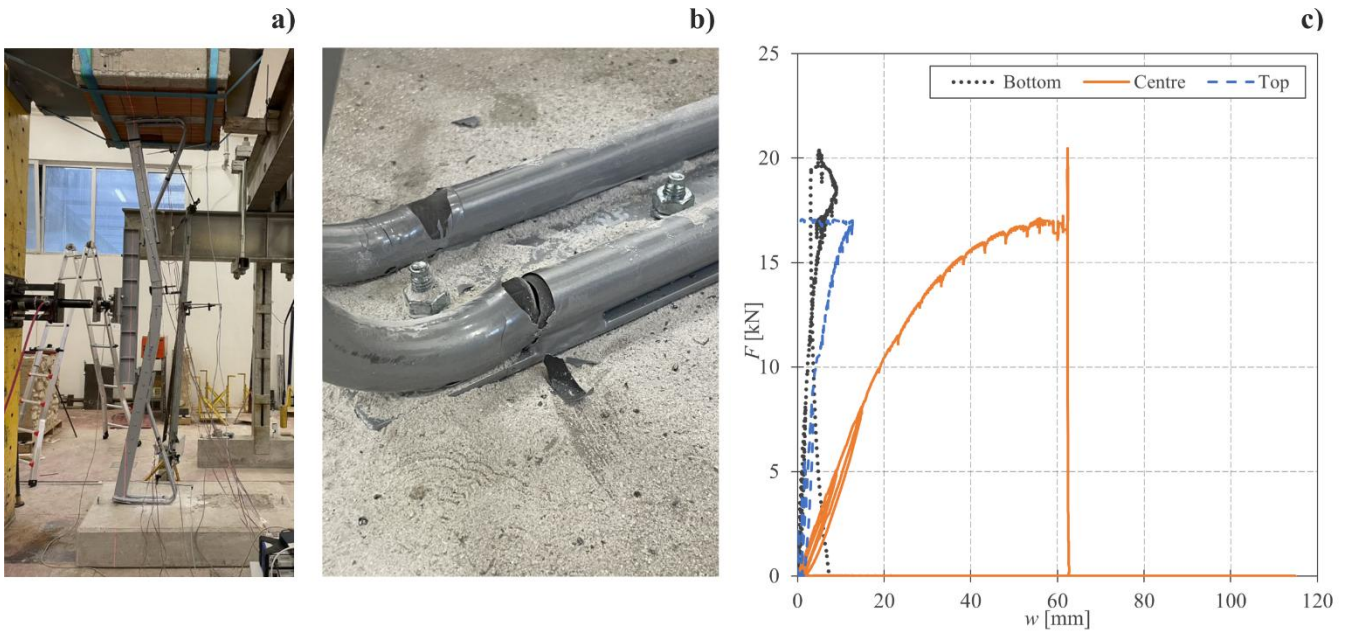


565

566 **Figure 31.** Test#5 results: **a)** Cantilever shape deformation; **b)** Force-displacement plot

567 The fifth test was carried out by placing the upper metal support plate under the hollow tiles of the
 568 ceiling floor and lowering the prestress force to 2 kN. The load bearing capacity was the same

569 recorded in test #4 and sliding mechanism was still observed. As for the LBDP prototype, the last
 570 test was performed to investigate the stud's strength. To compare the results, the same number, type
 571 and connector's position of the LBDP last test were reproduced. The result was the expected upright
 572 arched deformation shape and the highest maximum horizontal force equal to 21 kN was recorded.
 573 Hard damage in the inclined hollow tube-shaped profiles were observed (Figure 32).



574

575 **Figure 32.** Test#6 results: **a)** Arched shape deformation; **b)** Tube-shaped profiles collapse; **c)** Force-
 576 displacement plot

577 The main results from tests on self-supporting shelving units are summarized in Table 5. The
 578 capacity-to-demand ratio (C/D) was evaluated by assuming a demand force equal to the design
 579 force (23.8 kN, as previously defined), while the capacity was assumed as the experimental
 580 maximum recorded force. Restraints realized with elastomeric layer or elastomeric layer plus
 581 double-sided tape strips were not able to perform as expected, resulting in a reaction force
 582 sometimes lower than the prestress force (i.e., friction coefficient lower than the expected value for
 583 a rubber compound). Moreover, the designed arch mechanism never developed as expected in the
 584 FEM model of Figure 23 due to the curved shape of the stiffening triangular profiles. The circular
 585 hollow profiles composing such element of the upright behave not as pure truss beams, showing

586 lower stiffness and anticipated failure in bending (see Figure 32). Consequently, only in test #6 of
 587 the prototype UBDPs has drawn near the design load, highlighting the critical relevance of the
 588 boundary conditions and the negative influence of the curved stiffening triangular element, used by
 589 the producers to simplify the construction process. Nevertheless, the potentialities of the proposed
 590 solution were evident and C/D ratios larger than 1 are expected if care is given to the vulnerabilities
 591 shown by the experimental campaign.

592 **Table 5.** Summary of main results for self-supporting shelving units

Conditions	Test#	Position of the upper metal support plate	Base restraint type	Prestress force [kN]	Maximum force [kN]	Failure Mechanism	C/D [-]
LBDPs	1	Concrete joist	Elastomeric layer	4	6.5	Damage on profile's welded joints	0.3
	2	Hollow tiles	Elastomeric layer	2	2	Base sliding	0.1
	3	Hollow tiles	Elastomeric layer	4	2.9	Base sliding	0.1
	4	Hollow tiles	Elastomeric layer + 2M10 dowels	2	5	Base sliding	0.2
	5	Concrete joist + 3M10 dowels	3M10 dowels	0	8.5	Profile's arched deformation with local buckling	0.4
UBDPs	1	Concrete joist	Elastomeric layer	4	3	Base sliding	0.1
	2	Concrete joist	Elastomeric layer	8	3	Base sliding	0.1
	3	Concrete joist	Elastomeric layer + double- sided tape strips	8	6	Base sliding	0.3

4	Concrete joist	Elastomeric layer + 2M10 dowels	8	8.5	Top sliding	0.4
5	Hollow tiles	2M10 dowels	2	8.5	Top sliding	0.4
6	Concrete joist +3M10 dowels	3M10 dowels	0	21	Profile's arched deformation with damage on the hollow tube-shaped profiles	0.9

593 Conclusions

594 This paper describes a new life-saving furniture systems consisting of school desks and self-
595 supporting shelving units thought for school buildings that are not able to ensure seismic safety to
596 students and teachers. A wide experimental campaign was conducted with the aim of verifying the
597 efficiency of the proposed furniture and to characterize their ultimate capacities towards different
598 load and restraints conditions.

599 For the quasi-static test campaigns on desks, the new concepts showed promising characteristics,
600 namely, higher ductility and resilience in repeated tests. The dynamic test campaign gave
601 appreciable experimental evidences: *i)* the tabletops were never damaged during the impact,
602 regardless of the amount and type of load; *ii)* the horizontal and inner vertical steel frames only
603 deflect without collapsing; *iii)* the outer vertical frames were severely damaged only if the 600 kg
604 load was not centred otherwise they bent outwardly in the lower part with a ductile mechanism and
605 slid relatively at the base level. Some trial and error were necessary to iron out prototyping
606 imperfections evidenced by unexpected behaviours, leading to an optimised version of the proposed
607 desk.

608 For the self-supporting shelving unit, boundary conditions proved to be highly influential for both
609 capacity and deformation. The expected arch behaviour was partially achieved only when perfect
610 bond between horizontal plates and horizontal supporting surfaces, namely, floor and ceiling, was

611 performed, increasing the maximum reached load from 3 kN to 21 kN. The avoidance of sliding
612 between plates and supports will be key for the reliability and future commercialisation of this item.
613 Once the sliding of top and bottom restraints is avoided and the pure truss behaviour of the
614 stiffening triangular profiles granted, the design performance can be achieved. Nevertheless, the
615 tests suggested that the direction of work is promising, yet further detailing and prototyping is
616 needed.

617 The two prototypes showed improved capacity and additional features if compared with currently
618 on the market counterparts, using already in-house materials and manufacturing processes,
619 rendering them readily produceable at scale with minimal cost increase and additional precautions,
620 especially when the self-supporting shelf unit is considered.

621 ACKNOWLEDGMENTS

622 This research was carried out within the activities of the project “LIFE-SAVING Sustainable
623 Design of Anti-Seismic Furniture as Smart Life-Saving Systems during an Earthquake” funded by
624 the Italian Ministry of University and Research within the framework PON 2015-2018 in the
625 Specialization Area of “Design, Creativity and Made in Italy”, coordinated by the University of
626 Camerino. The Authors are grateful to the Principal Investigator Lucia Pietroni and the industrial
627 design research team at the University of Camerino (Jacopo Mascitti, Alesandro Di Stefano,
628 Daniele Galloppo, and Davide Paciotti). The Authors acknowledge the constructive interactions
629 with the industrial partners Camillo Sirianni s.a.s. (Soveria Mannelli, Italy) and Vastarredo s.r.l.
630 (Vasto, Italy) in the design stage and in developing the tested prototypes. The Authors are also
631 grateful to the technicians of the Laboratory of the University of L’Aquila, Edoardo Ciuffetelli and
632 Alfredo Peditto, for their valuable support during the tests. In addition, the Authors of the
633 University of Camerino acknowledge support in the subsequent developments of the research from
634 the European Union - NextGenerationEU, Mission 4, Component 2, under the Italian Ministry of

635 University and Research (MUR) National Innovation Ecosystem grant ECS00000041 - VITALITY
636 - CUPJ13C22000430001.

637

638 REFERENCES:

- 639 [1] Istituto Nazionale di Geofisica e Vulcanologia, Earthquake with magnitude of ML-MEDNET 5.4 on date 31-
640 10-2002 and time 11:33:00 (Italy) in region 1 km SW Bonefro (CB), (2002).
641 http://terremoti.ingv.it/en/finitesource_summary/36092321 (accessed 23 October 2024).
- 642 [2] Istituto Nazionale di Geofisica e Vulcanologia, Earthquake with magnitude of Mw 6.1 on date 06-04-2009 and
643 time 03:32:40 (Italy) in region 2 km SW L'Aquila (AQ), 2009. (2023).
644 http://terremoti.ingv.it/en/finitesource_summary/36092321 (accessed 20 October 2024).
- 645 [3] M.G. Di Francesco, R., Tiberii, La notte dell'Aquila [The Aquila night], Palermo, 2010.
- 646 [4] W. Salvatore, S. Caprilli, V. Barberi, Rapporto dei Danni Provocati dall'Evento Sismico del 6 Aprile sugli
647 Edifici Scolastici del Centro Storico dell'Aquila, 2009.
648 http://www.reluis.it/doc/pdf/Aquila/Rapporto_danni_scuole_Aquila.pdf.
- 649 [5] Perrone, D., Calvi, P.M., Nascimbene, R., Fischer, E.C., Magliulo, G., 2019. Seismic performance of non-
650 structural elements during the 2016 Central Italy earthquake. *Bull Earthquake Eng* 17, 5655–5677.
651 <https://doi.org/10.1007/s10518-018-0361-5>
- 652 [6] F. Braga, V. Manfredi, A. Masi, A. Salvatori, M. Vona, Performance of non-structural elements in RC buildings
653 during the L'Aquila, 2009 earthquake, *Bull. Earthq. Eng.* 9 (2011) 307–324. [https://doi.org/10.1007/s10518-](https://doi.org/10.1007/s10518-010-9205-7)
654 [010-9205-7](https://doi.org/10.1007/s10518-010-9205-7).
- 655 [7] T. MASATSUKI, S. Midorikawa, Simulation of Seismic Behavior of Furniture in High-rise Residential
656 Buildings due to Long-period Ground Motion, *J. JAEE.* 15 (2015) 6_1-6_11.
657 https://doi.org/10.5610/jaee.15.6_1.
- 658 [8] K. Meguro, D. Ito, Y. Sato, Efficiency Of Furniture Overturning Protection Devices During Earthquakes- A
659 Experimental and Numerical Study -, 14th World Conf. Earthq. Eng. (2008).
- 660 [9] Migliaccio, G. Analytical evaluation of stresses and strains in inhomogeneous non-prismatic beams undergoing
661 large deflections. *Acta Mech* 233, 2815–2827 (2022). <https://doi.org/10.1007/s00707-022-03247-x>
- 662 [10] Migliaccio, G. Analytical prediction of the cross-sectional shear flow in non-prismatic inhomogeneous
663 beamlike solids, *Thin-Walled Structures*, Volume 183, February 2023, 110384
664 <https://doi.org/10.1016/j.tws.2022.110384>
- 665 [11] Desroches, R., Migliaccio, G. and Royer-Carfagni, G. Structures That Can Be Made with Carbon Nanotube
666 Fibers but Not with Other Materials, *Journal of Engineering Mechanics* Volume 148, Issue 12

- 667 [https://doi.org/10.1061/\(ASCE\)EM.1943-7889.0002138](https://doi.org/10.1061/(ASCE)EM.1943-7889.0002138)
- 668 [12] G. International, Made in Bhutan The Earthquake Desk, (n.d.). [https://www.geohaz.org/all-projects/producing-](https://www.geohaz.org/all-projects/producing-affordable-earthquake-desks)
669 [affordable-earthquake-desks](https://www.geohaz.org/all-projects/producing-affordable-earthquake-desks).
- 670 [13] R. von Bereghy, LifeGuard Structures, (n.d.). www.lifeguardstructures.com.
- 671 [14] M. Fellin, M. Polidori, A. Ceccotti, Cross Laminated Timber furniture providing shelter during earthquakes.
672 Lifeshell public domain release., Interdiscip. Perspect. Built Environ. 2 (2022).
673 <https://doi.org/10.37947/ipbe.2022.vol2.2>.
- 674 [15] L. Pietroni, J. Mascitti, D. Galloppo, Life-saving furniture during an earthquake. Intelligent, interconnected and
675 interacting, AGATHÓN–International J. Archit. Art Des. 10 (2021) 218–229.
- 676 [16] D. Galloppo, J. Mascitti, L. Pietroni, Design strategies for the development of life-saving furniture systems in
677 the event of an earthquake, WIT Trans. Built Environ. 189 (2019) 67–77. <https://doi.org/10.2495/SAFE190071>.
- 678 [17] Magliulo, G., D’Angela, D., 2024. Seismic response and capacity of inelastic acceleration- sensitive
679 nonstructural elements subjected to building floor motions. Earthq Engng Struct Dyn eqe.4080.
680 <https://doi.org/10.1002/eqe.4080>
- 681 [18] Kazantzi, A.K., Miranda, E., Vamvatsikos, D., 2020. Strength- reduction factors for the design of light
682 nonstructural elements in buildings. Earthq Engng Struct Dyn 49, 1329–1343. <https://doi.org/10.1002/eqe.3292>
- 683 [19] Chen, M.C., Pantoli, E., Wang, X., Astroza, R., Ebrahimian, H., Hutchinson, T.C., Conte, J.P., Restrepo, J.I.,
684 Marin, C., Walsh, D., Bachman, R.E., Hoehler, M.S., Englekirk, R., Faghihi, M., 2016. Full-Scale Structural
685 and Nonstructural Building System Performance during Earthquakes: Part I – Specimen Description, Test
686 Protocol, and Structural Response. Earthquake Spectra 32(2), 737-770.
- 687 [20] Di Sarno, L., Magliulo, G., D’Angela, D., Cosenza, E., 2018. Experimental assessment of the seismic
688 performance of hospital cabinets using shake table testing. Earthquake Engineering and Structural Dynamics 1-
689 21.
- 690 [21] Pürgstaller, A., Gallo, P.Q., Pampanin, S., Bergmeister, K., 2020. Seismic demands on nonstructural
691 components anchored to concrete accounting for structure-fastener-nonstructural interaction (SFNI). Earthquake
692 Engineering and Structural Dynamics 49, 589-606.
- 693 [22] Filiatrault, A., 1991. Seismic evaluation of modular office furniture system. Earthquake Spectra 7(54), 524-541.
- 694 [23] Filiatrault, A., Kuan, S., Tremblay, R., 2004. Shake table testing of bookcase – partition wall systems. Canadian
695 Journal of Civil Engineering 31, 664-676.

- 696 [24] FEMA E-74. Reducing the Risks of Nonstructural Earthquake Damage – A Practical Guide. Federal
697 Emergency Management Agency, 2012
- 698 [25] Guide and checklist for Nonstructural Earthquake Hazards in California Schools. California Emergency
699 Management Agency, 2011.
- 700 [26] Case Studies of Seismic Nonstructural Retrofitting in School Facilities. National Institute for Educational
701 Policy Research, Study Group Report on the "Investigative Research for Promoting the Seismic Retrofitting of
702 School Facilities". Educational Facilities Research Center, 2005, Japan.
- 703 [27] Scozzese F., Zona A., Dall'Asta A. Glass-aluminium partition walls with high-damping rubber devices: seismic
704 design and numerical analyses. Buildings 2024, 14(8):2445. <https://doi.org/10.3390/buildings14082445>
- 705 [28] Ministry of Infrastructure and Transport. 2018. NTC 2018. Aggiornamento delle “Norme Tecniche per le
706 costruzioni” DM 17/01/2018 (in Italian).
- 707 [29] D’Angela, D., Magliulo, G., Di Salvatore, C., Zito, M., 2024. Seismic assessment and qualification of
708 acceleration-sensitive nonstructural elements through shake table testing: reliability of testing protocols and
709 reliability-targeted safety factors. Engineering Structures. <https://doi.org/10.1016/j.engstruct.2023.117271>